1965

Temperature distribution in thermal boundary layers (in free convection) using a modified Schlieren method

Philip Ling Chen

Department:

TEMPERATURE DISTRIBUTION IN THERMAL BOUNDARY LAYERS (IN FREE CONVECTION) USING A MODIFIED SCHLIEREN METHOD

BY

PHILIP LING CHEN

A

THESIS

submitted to the faculty of the

UNIVERSITY OF MISSOURI AT ROLLA

in partial fulfillment of the work required for the

Degree of

MASTER OF SCIENCE IN MECHANICAL ENGINEERING

Rolla, Missouri

1965

Approved by

E. R. Remington Jr. (Advisor) John C. Nelson

H. J. Sauer Jr. Robert D. Way

ACKNOWLEDGEMENT

The author wishes to express his appreciation to Professor C. R. Remington, Jr., advisor in this work, and to Professor L. G. Rhea for his valuable advice and criticism during the course of this investigation. He is also indebted to Mr. Lee N. Anderson for his assistance in the construction of the apparatus.

ABSTRACT

A simple optical apparatus, the Schlieren interferometer, was constructed for the quantitative investigation of free convection heat transfer from solid bodies. The photographic results, checked by using thermocouples, were used in evaluating the temperature distribution, the key to the solution of these problems. Interpretation of the photographic results was made using the simple calculation for the conventional interferogram and the Dale-Gladstone law. Although the experiments were limited to a heated flat plate and a heated wire, two dimensional test pieces of irregular configuration can be investigated by the same apparatus with simple modifications.

The photographs of the conventional Schlieren, the color Schlieren, and the modified Schlieren were compared using the same apparatus and they reveal that the Schlieren interferometer is a powerful tool for compressible fluid flow investigation.

TABLE OF CONTENTS

LIST OF FIGURES AND TABLES

Tables

I. REVIEW OF LITERATURE AND SCIENTIFIC BACKGROUND

Heat transfer by convection is the exchange of energy between moving particles of the fluid or between these and surfaces of different temperature. It is obvious that the transfer of energy depends upon the motion of the fluid and is governed by the laws of fluid dynamics in addition to the laws of heat conduction. The change of internal energy is also affected at the same time. Hence, heat convection is a very complex process. As a matter of fact, the convective heat transfer coefficient, h, is a function of many variables, such as shape, dimensions of the surface, roughness, direction, velocity of the flow, surface temperature, density, viscosity, specific heat, and the thermal conductivity of the fluid.[1*]

The differential equations which describe convective heat transfer belong to the most difficult class of theoretical physics, and only for a very few simple cases has it been possible to solve them. The other methods available for the evaluation of convective heat transfer coefficients are dimensional analysis combined with experiments, approximate analyses of the boundary layer by integral methods, and the analogy between heat, mass, and momentum transfer.[2]

---

*Superscript numbers indicate specific references listed in the Bibliography.

All four of these techniques have contributed to the understanding of convective heat transfer. Yet, no single method can solve all the problems because each one has limitations which restrict its scope of application.

So far, in heat transfer by convection, progress has been especially dependent upon an intimate cross-fertilization between the analytical and empirical branches; the experimental results being most fruitfully interpreted in terms of theoretical reasoning, and the analyses in turn suggest critical and illuminating experiments which further amplify and strengthen the theory.

Among the methods now in use for convective heat transfer experiments, optical methods are the most favorable type for they furnish results about the flow without disturbing it. Many of the optical methods employed in the examination of thermal convective currents or compressible gas flows are based on one of the following two physical phenomena; 1) the speed of light depends on the index of refraction of the medium through which it passes, and the index of refraction of a gas in turn depends upon its density, and 2) light passing through a density gradient in a gas (and therefore through a gradient in index of refraction) is deflected in the same manner as though it were passing through a prism.

Generally, the optical methods in common use are the

Interferometer, the Schlieren, and Shadowgraph. The Interferometer measures changes of density directly, and is relatively the most accurate and expensive instrument. The Schlieren method measures density gradients and it is theoretically adaptable to quantitative use, but it is inferior to the Interferometer in this respect, and its greatest utility is in giving an easy interpretable picture of the flow field together with a rough picture of the density variation in the flow. The Shadowgraph method measures the second derivative of the density, that is, the first derivative of the density gradient. Therefore, it makes visible only those parts of the flow where the density gradients change very rapidly, and it has found its greatest utility in the study of shock waves. Because of its simple construction and because it is easy to operate, the shadowgraph is the least expensive method. Each method therefore has its own useful niche in experimental work, and the choice of method depends on the nature of the investigation.[3]

1) Schlieren Method:

The Schlieren method was chosen for the thermal boundary layer investigation in the following experiments because it is relatively simple and inexpensive. Also, it is less sensitive, than the interferometer, to minor adjustments and slight imperfections in the optical components. With suitable design modifications the Schlieren

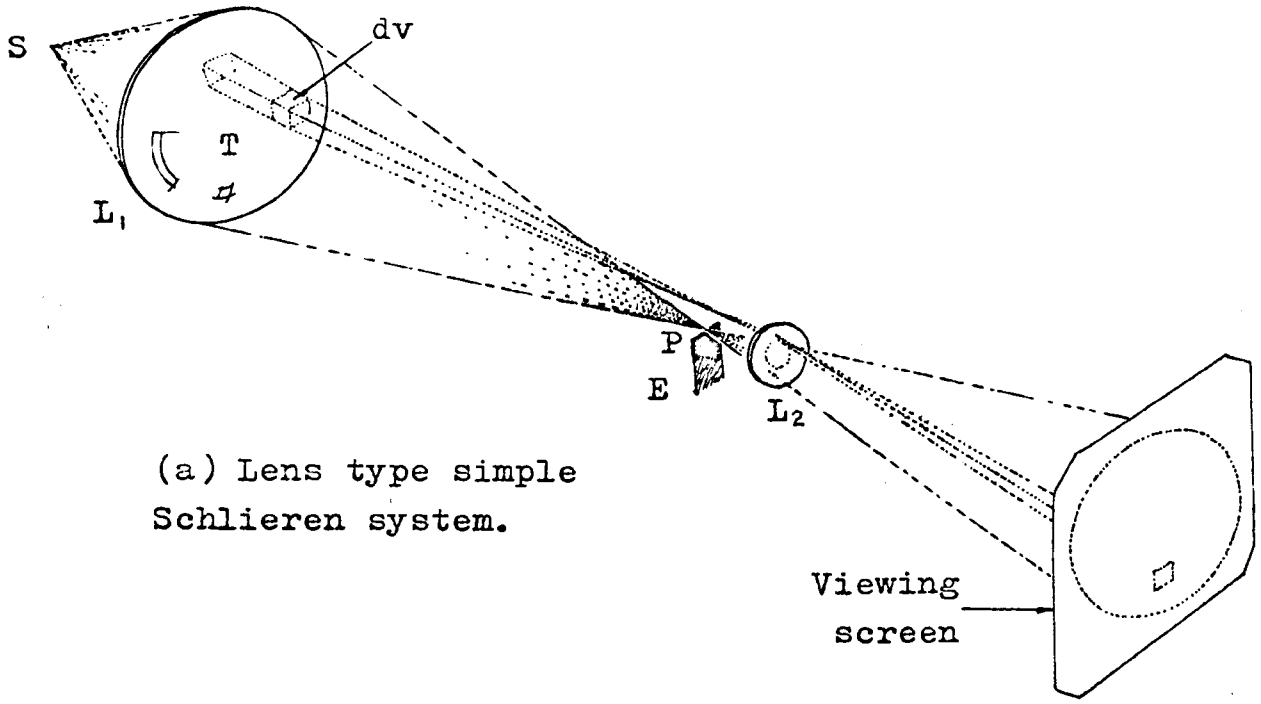

(a) Lens type simple Schlieren system.

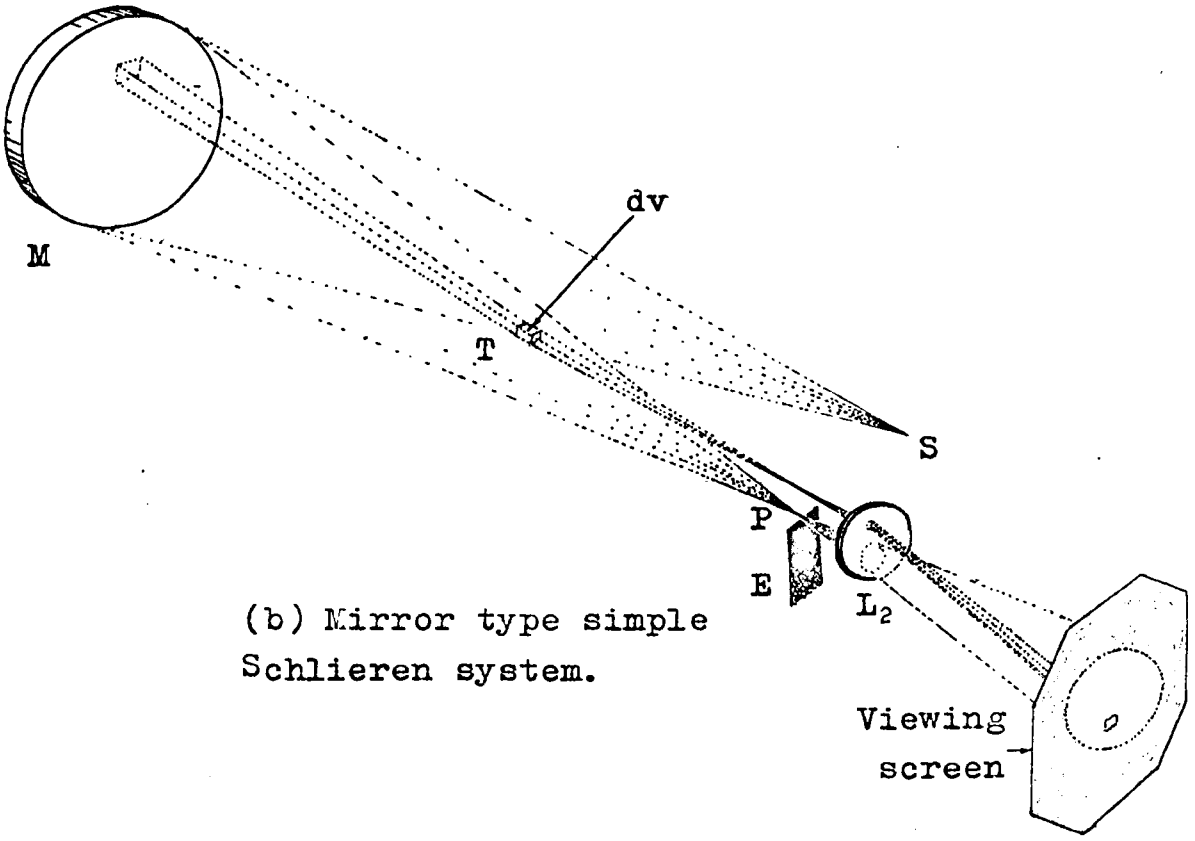

(b) Mirror type simple Schlieren system.

Fig. 1. Simple Schlieren.

can be used for quantitative investigations. This is known as Schlieren interferometry and will be discussed later.

The fundamental principle of conventional Schlieren dates back about 105 years. At that time Foucault devised a test, which now bears his name, for observing the surface configuration of a concave telescope mirror. Though in the tests Foucault probably observed what were apparently heat waves passing in front of his mirror surface, it remained for Topler to realize the real significance of this additional phenomenon. Since the latter's publication in 1864, the method has been often referred to as the Topler Schlieren method.

The operating principle of a simple Schlieren system can be best described with reference to Fig. 1. Light from an illuminated pinhole S, is allowed to fall upon lens L_1 (or mirror M) and then converged to the image point at P. If the eye is placed slightly behind the image point, as in the Foucault test, the lens L_1 (or mirror M) will appear as a uniformly illuminated field. In usual practice, however, a lens L_2 is substituted for the eye, this lens focusing the striation upon a viewing screen or upon a photographic plate. If the knife-edge E is then moved vertically across the image point until all the rays passing through that image are obscured, the field as viewed upon the screen will be uniformly dark.

The next consideration is the effect of introducing air into a very small element of volume dv (Fig. 1). The index of refraction n, of this air is different from that of the surrounding air n_o for which the knife-edge has been adjusted to produce a uniformly dark field upon the viewing screen. A light ray passing through the volume dv will be refracted, and it will no longer proceed along its original path, except for the singular instance where the gradient or change in the index of refraction which is a function of the space position, is parallel to that light ray.

If the gradient of n through the refraction is so directionally constituted that the light ray is refracted in a counterclockwise manner, this ray will no longer pass through the image point P but will travel above it. Hence, this ray will not be obscured by the knife-edge but will pass on to the screen. There it will illuminate a point corresponding to the location of the elementary volume dv. Thus for every point in the region T for which a similar refraction takes place, there will be a corresponding point illuminated on the viewing screen. The composite of all such points forms the image of the phenomenon being investigated.

If the refraction in the elementary volume dv is in a clockwise direction, the rays will be bent down toward the base of the knife-edge, and the corresponding points on the viewing screen will be dark.

In making the vertical adjustment of the knife-edge when no striation is present in the region T, it is usually desirable to allow some of the rays to pass over the knife-edge in order to produce a uniform low background illumination. The presence of this background makes it possible to see more clearly in silhouette or outline the objects or models used in producing the free convection phenomena. Thus, referred to the earlier paragraphs about the refraction produced by the elementary volume dv, a counterclockwise bending of a light ray will produce an increase in illumination at the corresponding screen point; a clockwise bending will produce a decrease in screen illumination.[4]

2) Color Schlieren:

For color Schlieren the light is not monochromatic but rather it is a series of light points or strips of different colors such as a spectrum. The different color light sources impinge on the lens L_1 (or concave mirror M) at slightly different angles. This effect produces a different light deflection angle due to different density gradient in dv, making the image on the screen appear in a different color. The light strip was cut off by means of a slit (one image color strip in width) instead of the conventional knife edge. If the test section is undisturbed, only one light strip of the image can pass through the slit, and the screen appears to be uniform monochromatic light. The color of the screen background can be

selected by moving the slit S to allow the desired color light strip to pass through.[5]

Since the index of refraction of different light colors is different, the longer the wavelength, the lower the refractive index; and the shorter the wavelength, the higher the refractive index. In interpreting the color Schlieren it is necessary to make individual calculations for each color.

Theoretically, the color Schlieren is superior to the conventional Schlieren for it gives a color picture of the light deflection. The different light deflections can be read directly by virtue of the different colors, while light deflections on the conventional Schlieren picture should be read by a densitometer.

Practically, the Fraunhoffer diffraction, due to the cut-off slit S, would blur the image on the screen and decrease the definition of the image. Because of this fact, the slit S should be made as wide as possible, since the wider the slit S the lower the blur. An undesired decrease in sensitivity also occurred. The width of the slit S should be determined experimentally according to the sensitivity requirement and blur tolerance for the investigation.

3) Schlieren Interferometry:

In 1956, Edward B. Temple suggested a simple modification of the conventional Schlieren system to achieve the function of the Mach-Zehnder Interferometer. The principle of this modification is that a plane wave front in a collimated beam of light is distorted in the passage through a region of variable density, and as a result a variable phase distribution is produced in an exit plane which lies just beyond the disturbance and is perpendicular to the direction of propagation of the collimated beam (optical axis). This phase distribution, ordinarily invisible because of the tremendous rapidity of optical oscillations, can be converted to an intensity distribution in which the maxima and minima of intensity correspond to points in the exit plane where the optical path length differs from that in an undisturbed portion of this plane (free-field) by an integral multiple of half a wavelength. This can be done in a conventional Schlieren system by forming an image of the exit (object) plane with a convex lens (or concave mirror), and then inserting a small absorbing object or other appropriate modification in the focal plane in such a way as to block the central maximum of the Fraunhoffer pattern due to the free field.

Very little disturbance light is cut off in the process since this light is refracted and does not go through the focal point. The blocking of free-field light sets up a

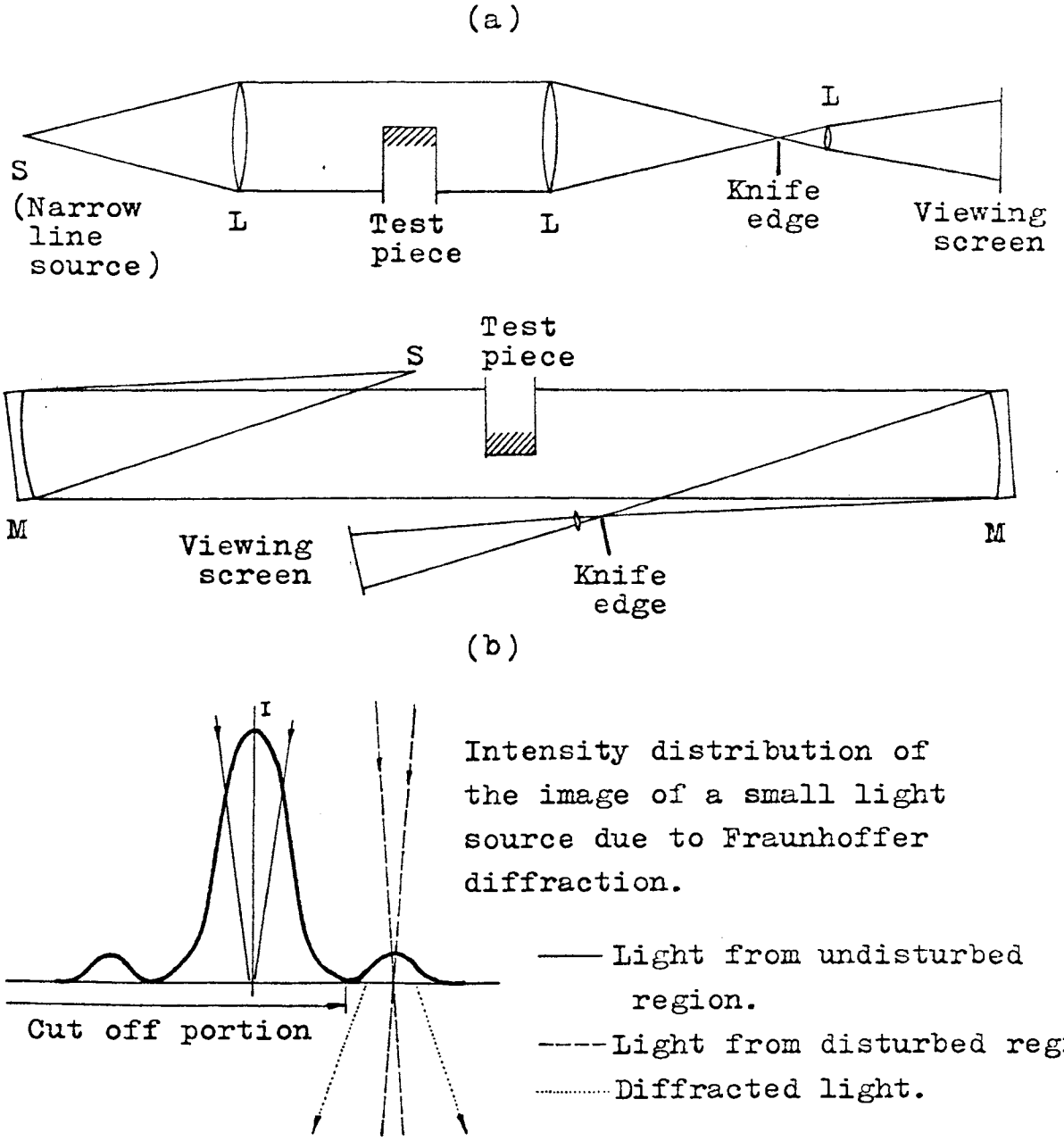

Fig. 2. Principle of Schlieren interferometry.
(a) Lens type and mirror type Schlieren interferometer.
(b) Fraunhoffer diffraction pattern of the light source image. Diffracted light from escaped portion of light source image of undisturbed region combined with disturbed light which causes interference.

diffraction process which causes this light to spread into the bordering disturbance image. The resulting interference produces the intensity band system.

If the disturbance is two-dimensional, with density gradient vectors perpendicular to the optical axis, the measurement of the phase distribution is equivalent to a measurement of density. This is by virture of the Dale-Gladstone law, the local index of refraction minus one is proportional to the local gas density. Measurements which have heretofore required the use of a Mach-Zehnder Interferometer can, therefore, be made in a conventional Schlieren system.[6] The schematic diagram of the principle of the Schlieren interferometry is shown on the last page. (Fig. 2)

Interpretation of Interferograms:

Assuming that a monochromatic line source of wave length λ is collimated by the lens L_1 (or concave mirror M_1) as shown in Fig. 2 , passing through the test section, the test section would be uniformly illuminated if there is no disturbance throughout the optical system.

Once the test piece in the test section is heated, the air density in the thermal boundary layer changes which in turn changes its refraction index. The interference fringes formed according to the aforementioned principle are practically a picture of iso-optical path length difference

lines. At the lines of maximum light intensity the difference in optical path length is found for both paths by

$$\int_0^L n\,dz = OPL,$$

where L is the length of the test section, n is the index of refraction, dz is the differential of the optical axis z, and OPL is the optical path length. The optical path length difference OPLD is $N\lambda$, where N = 0,1,2, denoting the fringe order. At a point of minimum light intensity, $OPLD = (N + 1/2)\lambda$.

With flow containing gradients in density, and therefore gradients in the index of refraction, a fringe pattern is formed such that

$$\int_0^L n\,dz = \int_0^L (1 + K\rho)\,dz$$

is constant on any one fringe and changes by λ for adjacent fringes. K is the Dale-Gladstone constant. Thus for two dimensional flow, $\rho = \rho(x,y)$, and $(1 + K\rho)L$ is constant along any one fringe and if ρ is known on any fringe it is known on all fringes throughout the field.[7]

II. EQUIPMENT AND APPARATUS

The optical instrument which was used in this investigation was the twin-mirror Schlieren system with the optical set up as shown in Fig. 3. Each part was constructed and assembled by the author. Many hours were spent in the testing, calibration, and modification of the complete assembly. It is best to describe the instrument by parts according to their functions. The main parts are the chassis, the light source system, the diagonal mirrors, the image cut-off device, the test piece holder, and the viewing and/or recording devices.

1) Chassis: (Fig. 5.)

The chassis of the complete Schlieren system was made of plywood. It was a box 96 inches long and 8 inches in height and depth. The length of the box was determined by the focal length of the concave mirrors. The minimum length of the twin-mirror Schlieren system was twice the focal length plus the length of the test section. The box with all its attachments was set on a rigid table. Because of the integral assembly on one rigid chassis, the experiments were successfully accomplished with little or no adjustment between runs. The parabolic concave mirrors were mounted on adjustable mounts face to face at the ends of the box.

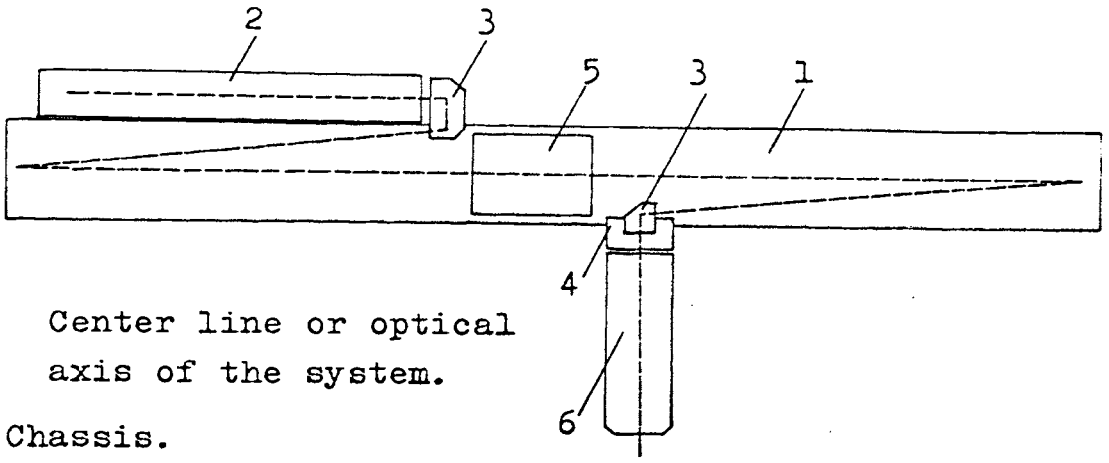

1. Chassis.
2. Light source system.
3. Diagonal mirror.
4. Image cut-off device.
5. Test piece holder.
6. Viewing and recording device.

Fig. 3. Main parts of a twin-mirror Schlieren system.

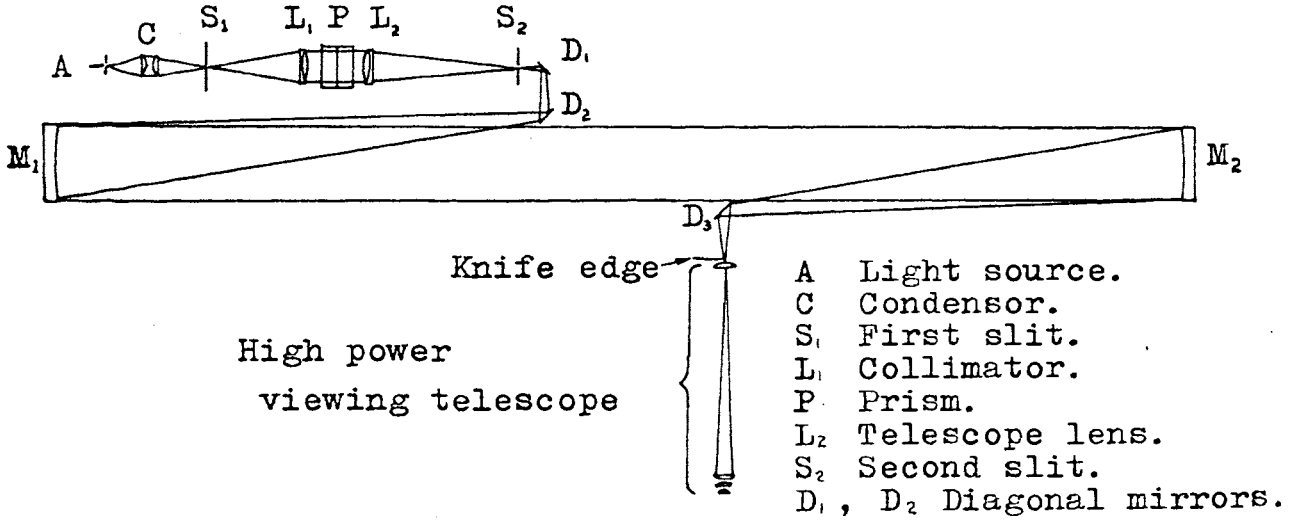

A Light source.
C Condensor.
S_1 First slit.
L_1 Collimator.
P Prism.
L_2 Telescope lens.
S_2 Second slit.
D_1, D_2 Diagonal mirrors.

Fig. 4. Schematic diagram of twin-mirror Schlieren system.

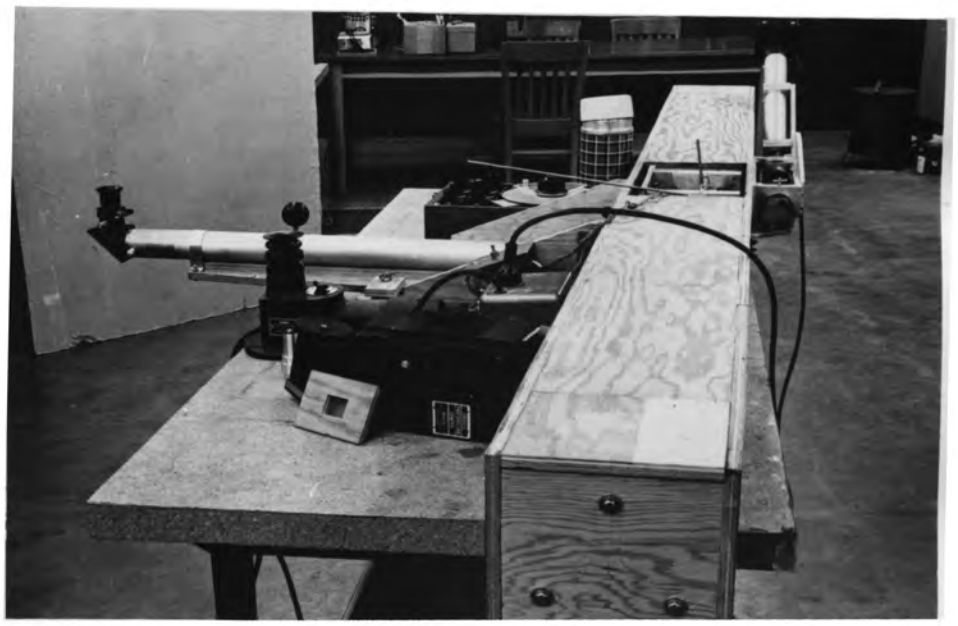

Fig. 5. The complete Schlieren system.

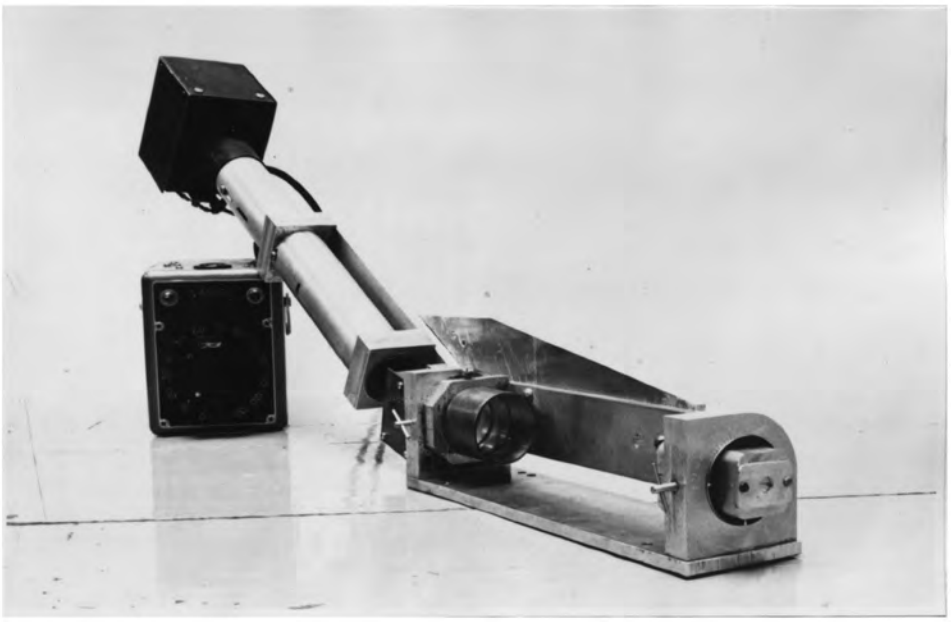

Fig. 6. The light source system.

2) Light Source System: (Fig. 3,4, & 6)

A GE 1034 light bulb served as the light source energized by 12 volts AC supplied through a variable voltage transformer. The light from the filament of the bulb was focused by the condenser system C. This produced an image on the first slit which allowed only the narrow and uniform central portion of the image light to penetrate the slit. The pencil light from the first slit was impinged on the collimating lens L_1 which was exactly one focal length from the slit S_1. The light left the collimating lens in parallel rays. This parallel light was spread by a prism P which formed a spectrum at the focus of a telescope objective lens L_2. This was exactly the same principle as a prism spectroscope.

This light source, with its continuous color spectrum can be used in many different ways; the whole spectrum can be used as the light source for a color Schlieren; a narrow strip of the spectrum can be used as a monochromatic light source for a conventional Schlieren; and an extremely narrow monochromatic strip from the spectrum made a light source for Schlieren interferometry. In order to change the direction of the light source slit S_2 and to achieve maximum sensitivity, the light source system was turned from a horizontal to a vertical position along the optical axis of the telescope objective lens L_2. Every optical part in this system was made adjustable along its optical axis, and the

slits were also made adjustable for agreement in all the components. The complete light source system was made as a separate rigid unit which could be quickly installed or removed by four wing nuts for necessary adjustment.

3) Diagonal Mirrors: (Fig. 3 & 4)

In order to make the complete Schlieren system compact, three front surface diagonal mirrors D_1, D_2 and D_3 were used; D_1 and D_2 were used to guide the light from the light source slit S_2 through a hole in the back of the box to the first concave mirror M_1 set at an angle of 2°20'. This angle is not critical, but it was made as small as possible to minimize aberration. The third front surface diagonal mirror D_3 was used to reflect the light from the second concave mirror M_2 to the front of the box through another hole. This formed an identical image of the light source slit S_2 at the knife-edge plane or the focal plane of the second concave mirror M_2. The third diagonal mirror D_3 was mounted on the movable let of the image cut-off device for focusing.

4) Image Cut-off Device: (Fig. 3, 4 & 7)

The basic mounting of the image cut-off device or the knife-edge moving device was a microscope slide moving stage, which affected the vertical movement of the knife-edge and the focusing diagonal mirror D_3 which was mounted on the horizontal leg. In addition to the vertical move-

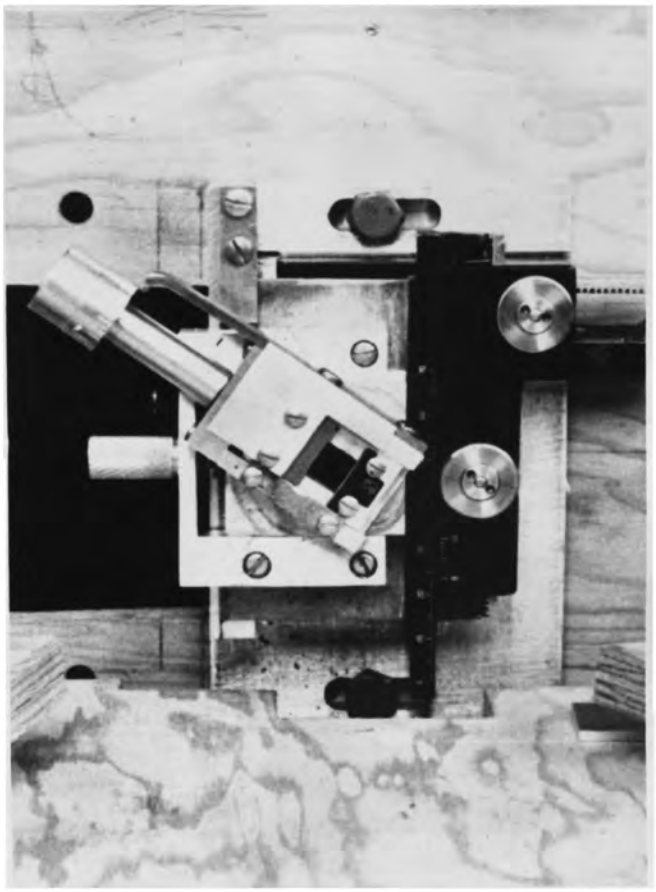

Fig. 7. The image cut off device.

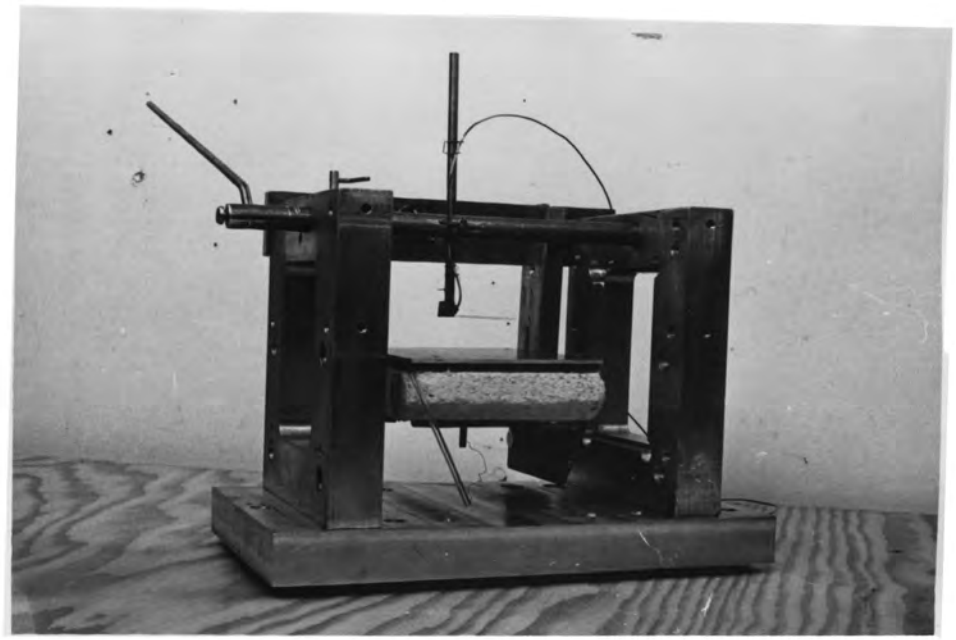

Fig. 8. The test piece and the test piece holder.

ment of the knife-edge, three more adjustments were added to the device; horizontal, rotational, and inclining-transversal motion. Therefore, the knife edge could be moved to any point and adjusted in any direction minutely on the focal plane of the second concave mirror M_2.

5) Test-piece holder: (Fig. 8)

The test piece holder was made of an one inch thick aluminum slab. It could hold test pieces of different sizes up to widths of six inches, at any angle. A built-in thermocouple holder was adjusted with the aid of the high power viewing telescope to measure the temperature at different positions on the test piece, or at any distance from the test piece surface. The complete holder could be removed from the test section directly for adjustment or changing the test pieces.

6) Viewing and Recording Devices:

Three telescopes and a recording camera were used in the experiments.

A) Telescopes: (Fig. 9)

a) A 8 x 57 elbow telescope was used for whole field viewing purposes. It was excellent for qualitative checking or for demonstration.

b) A 21 x 30 astronomical quality viewing telescope was used for quantitative measurements.

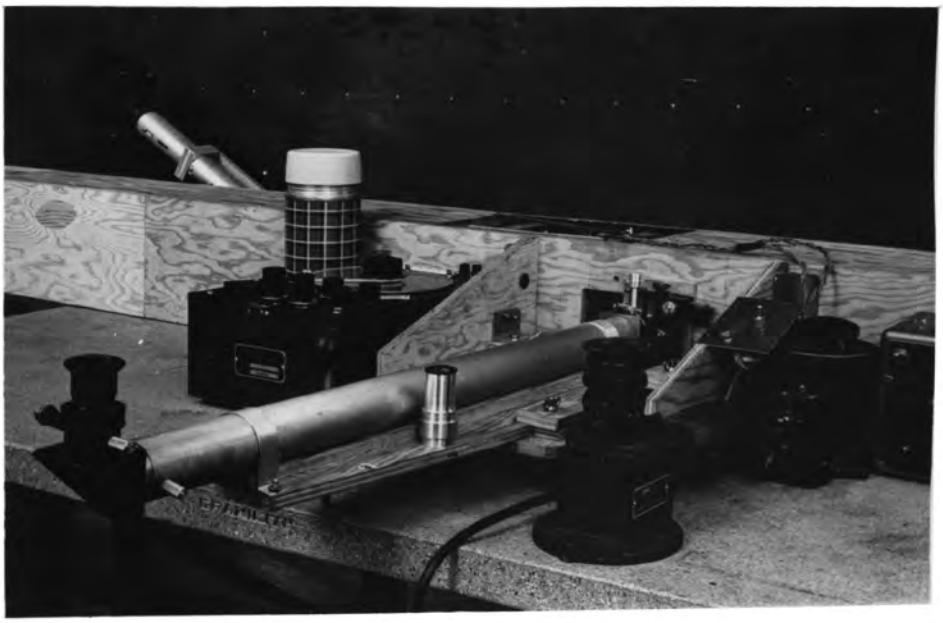

Fig. 9. The instruments and the telescopes.

c) A 5 x 11 calibration telescope was used for checking the parallelism of the light source image to the knife edge during adjustment.

B) Recording Camera: (Fig. 10)

The recording camera used was a photorecording camera obtained from a surplus house. Its lens system was removed and the shutter was mounted in front of the high power telescope objective lens. Hence the telescope objective lens served as a camera lens with a 31 inch focal length. The image on the film was about two thirds of the actual size.

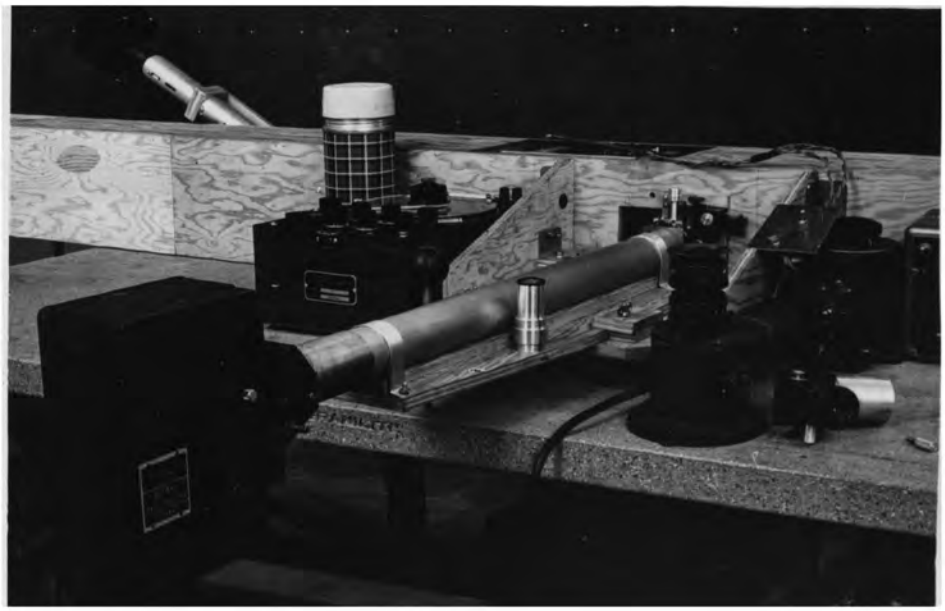

Fig. 10. The recording camera in working position.

TABLE I. OPTICAL PARTS

Name	Symbol	Specification
Light Source System:		
Light bulb	A	G-E 1034 Automobile light bulb
Condenser	C	Two achromatic lenses. D = 38mm f.l. = 130mm.
First slit	S_1	0.25mm wide, 10mm long.
Collimator	L_1	Achromatic objective lens. D = 35mm f.l. = 178mm.
Prism	P	Light flint glass prism. 32mm x 49mm x 35mm.
Telescope objective lens	L_2	Achromatic objective lens. D = 48mm f.l. = 343mm.
Second slit	S_2	5mm wide 7mm long.
	S_2'	0.3mm wide 7mm long.
	S_2''	0.05mm wide 6mm long.
Diagonal Mirrors:	D_1, D_2, D_3	Front surface mirrors. 1/4-wave flatness.
Parabolic concave mirrors:	M_1, M_2	Astronomical telescope mirrors, aluminized and overcoated, 1/4 wave or better, D = 4" f.l. = 45"
Viewing and Recording Device:		
Elbow telescope	T_1	8 x 57 surplus elbow telescope.

TABLE I. (continued)

High power telescope	T_2	21 x 30 astronomical telescope with scale on field lens of eyepiece.
Calibration telescope	T_3	5 x 11 astronomical telescope with 12.5mm e.f.l. Ramsden eyepiece.
Recording camera	R	modified Graflex recording camera f.l. = 778mm.100' 35mm film loading capacity.

III. EXPERIMENTAL INVESTIGATION

In this thesis, the temperature distribution in the thermal boundary layer was investigated mainly by Schlieren interferometry, because it furnished the easy interpretable information both in visual results and photographic results. The conventional Schlieren and the color Schlieren are also briefly discussed for comparative purposes.

1) Conventional Schlieren:

The instrument was adjusted according to the method described in Appendix I, using a narrow slit, S_2, 0.3 mm wide and 7 mm long as the monochromatic light source. (Refer to Table I) The light green color was chosen from the spectrum for visual comfort.

As the power of the light source was applied, the test section was brightly and evenly illuminated. If the knife edge is well adjusted such that it is exactly parallel to the light source image, and in the same focal plane, the test section would darken evenly as the knife edge was moved to cut off the light beam. For qualitative purpose and maximum sensitivity the knife edge was adjusted so as to intercept about half the available light. Then the test section looked uniformly illuminated by that portion of the light escaping the knife edge. When the test piece was heated in the test section, a bright region was produced on one side and a dark region appeared on the opposite side

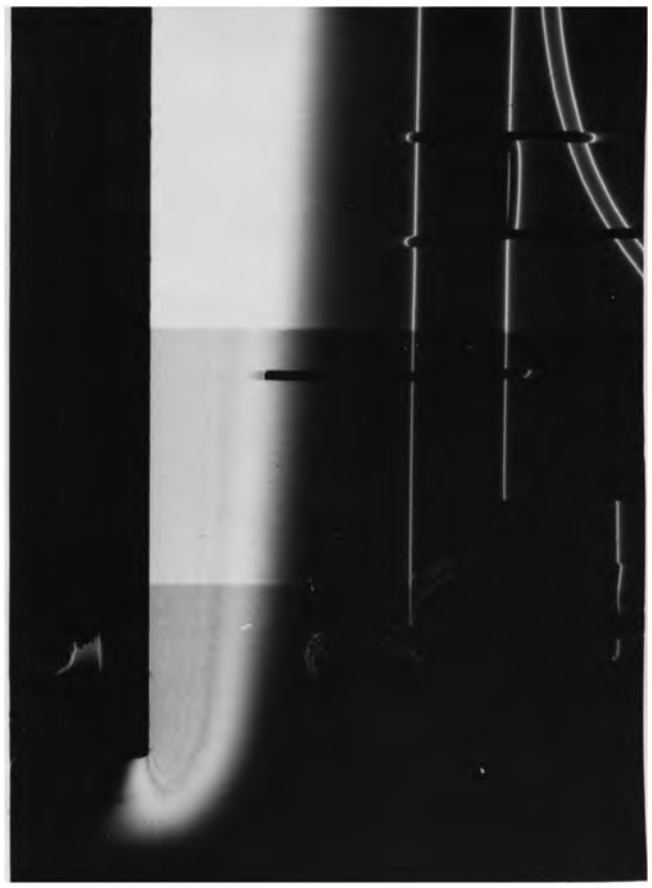

Fig. 11. Conventional Schlieren photograph of heated vertical plate. The different exposures show different boundary layer thicknesses. Width of light source slit = 0.3 mm.

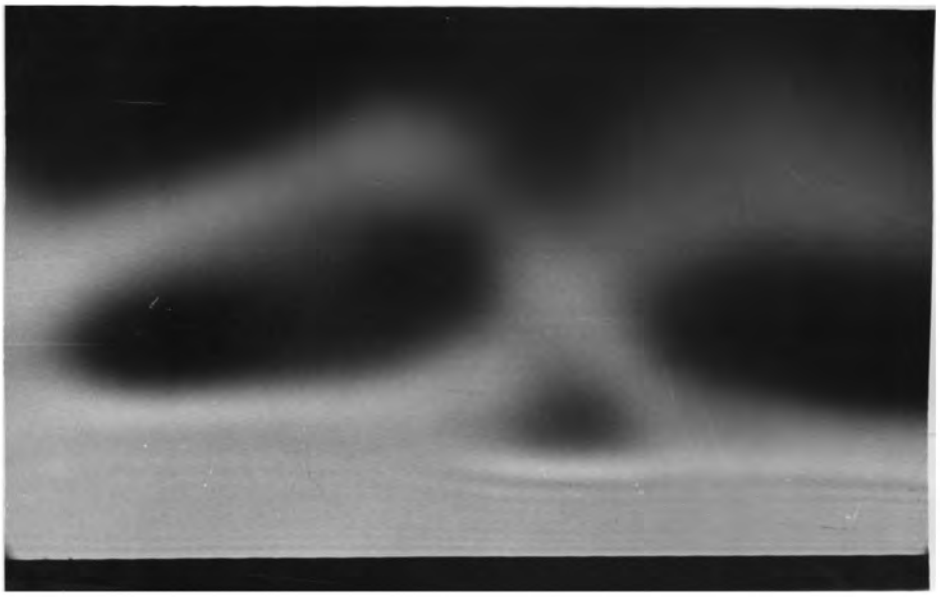

Fig. 12. Conventional Schlieren photograph of heated horizontal plate with hot surface upward. Width of light source slit = 0.3 mm.

according to the theory mentioned in the review of literature. The deflection of light in this manner is very critical, because if the deflection angle is larger than the critical angle the background illumination of the test section would remain constant. The critical angle of deflection is discussed in Appendix II. Therefore, the higher density gradient is not detectable in the Schlieren when operating at maximum sensitivity. However, it was useful in the visual observation of thermal boundary layer thicknesses. It should be noticed that the photographic results were not reliable because the different boundary layer thicknesses were obtained at different exposure as shown in Fig. 11.

Visual results were obtained by locating the boundary layer thickness on the scale in the eyepiece of the high power telescope. Each small division represented 0.30 mm or 0.0118 inches. The Schlieren patterns were also observed in photographs as shown in Fig. 11, 12.

2) Color Schlieren:

The conventional monochromatic Schlieren system was easily converted to a color Schlieren by changing the narrow slit, S_2' to a wide slit, S_2, (refer to Fig. 4 and Table I) and by changing the knife edge to a narrow slit.

If a Ronchi-ruling (50 lines per inch) is placed in front of the wide slit S_2, the spectrum is then cut into

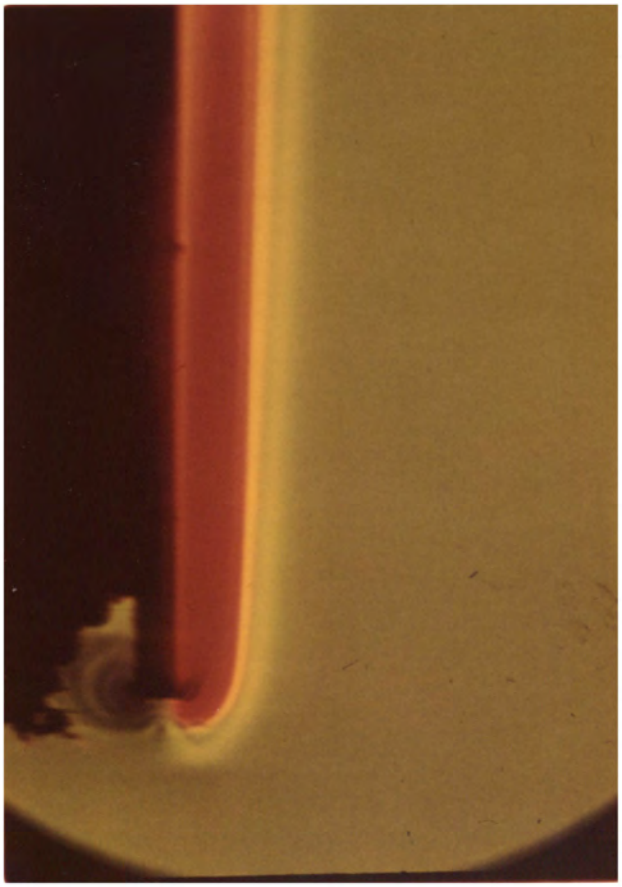

Fig. 13. Color Schlieren photograph of a heated vertical plate.

many evenly divided narrow strips of different colors. With this kind of modification, the different deflections, one fiftieth of an inch apart, are separated by dark lines. This produced a very rough view of iso-deflection lines. But, when these lines were not parallel to the slit, their position was not reliable, because the Schlieren system has maximum sensitivity only when the density gradient is perpendicular to the cut-off edge or slit. When the knife edge was replaced by a narrow slit, Fraunhoffer diffraction of the light caused interference blurring the image. This effect was decreased by using a 25 lines per inch metal wire grating with a slit 1.2 mm wide. The color Schlieren pattern is shown in Fig. 13.

3) Schlieren Interferometry:

If the slit S_2 (Refer to Fig. 4 and Table I) is made 0.05 mm or less, the Schlieren system can be converted into a Schlieren interferometer. When the parallelism of the cut-off edge and light source image was checked, interference fringes appeared around the heated test piece. One thing that should be mentioned is that the knife-edge must just cut off the image of the undisturbed light beam. This cut off sets up a diffraction process which causes the undisturbed light to spread into the disturbed image and cause interference. The proper image cut-off amount can be examined through the viewing telescope to see that only the undisturbed field is darkened. The interference fringes

Fig. 14. Probing the convective boundary layer with a thermocouple.

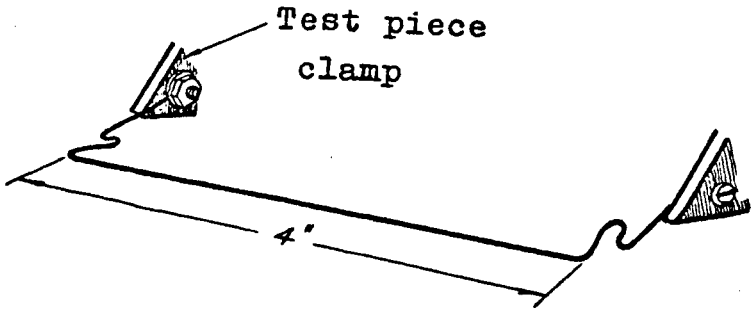

(a)

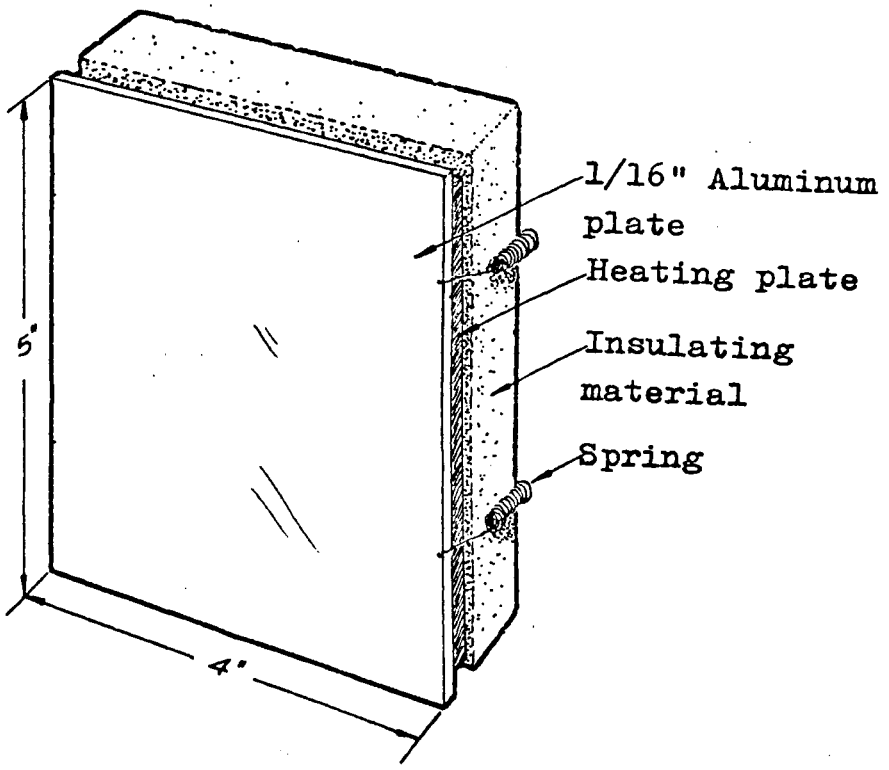

(b)

Fig.15. Test pieces, (a) horizontal heated wire, and (b) heated flat plate.

(Fig.14) represent the iso-index of refraction lines, which can be converted to iso-density lines by the Dale-Gladstone law. For constant pressure, the iso-density lines are also equivalent to isothermal lines.

Test Pieces: (Fig.15)

In these experiments the test pieces for investigating the free convective thermal boundary layers were a flat plate and a straight horizontal wire. The test pieces were placed parallel to the collimated or parallel light ray. Because the thickness of the thermal boundary layer is small compared to the length of the plate or wire, the effect of the ends was almost negligible. The test piece was therefore assumed to be two dimensional at steady state condition.

a) Horizontal Heated Wire:

A 0.03 inch diameter straight resistance wire, 4 inches long, was heated by passing alternating current through it. The temperature of the wire was controlled by varying the voltage. The surface temperature was checked by a small thermocouple along the wire. It appeared that the temperature was very uniform and the temperature difference between different points was negligible.

b) Heated Plate:

A 4" x 5" aluminum plate, 1/16 inch thick was heated by pressing it with springs against an electric heater.

The temperatures of the surface at various locations were measured under steady state conditions with a thermocouple. The maximum variation in temperature over the surface was less than 3°F.

Thermocouple: (Fig.14)

A 28 gage copper-constantan thermocouple was used. The wires of the thermocouple were ground, using fine emery cloth, to the size of less than 0.004 inch to avoid conduction losses and to avoid disturbing the boundary layer. Many different lengths of thermocouples were tried. It appears that the length of this thermocouple should not be less than 1.5 inches. A 1 3/4 inch long thermocouple was used to take data very close to the temperatures calculated from both visual and photographic results. One of the examples is shown in Fig.16.

Procedure:

In these experiments, before taking photographs of the interference patterns, much visual data were observed and these were checked with the sensitive thermocouple placed parallel to the isothermal surface. The positions of the fringes and the thermocouple were directly read through the viewing telescope.

The thermocouple readings were very close to the optical observations. Therefore, the error due to radiation was assumed to be negligible compared to the experi-

Fig. 16 . Visual result of heated vertical plate.

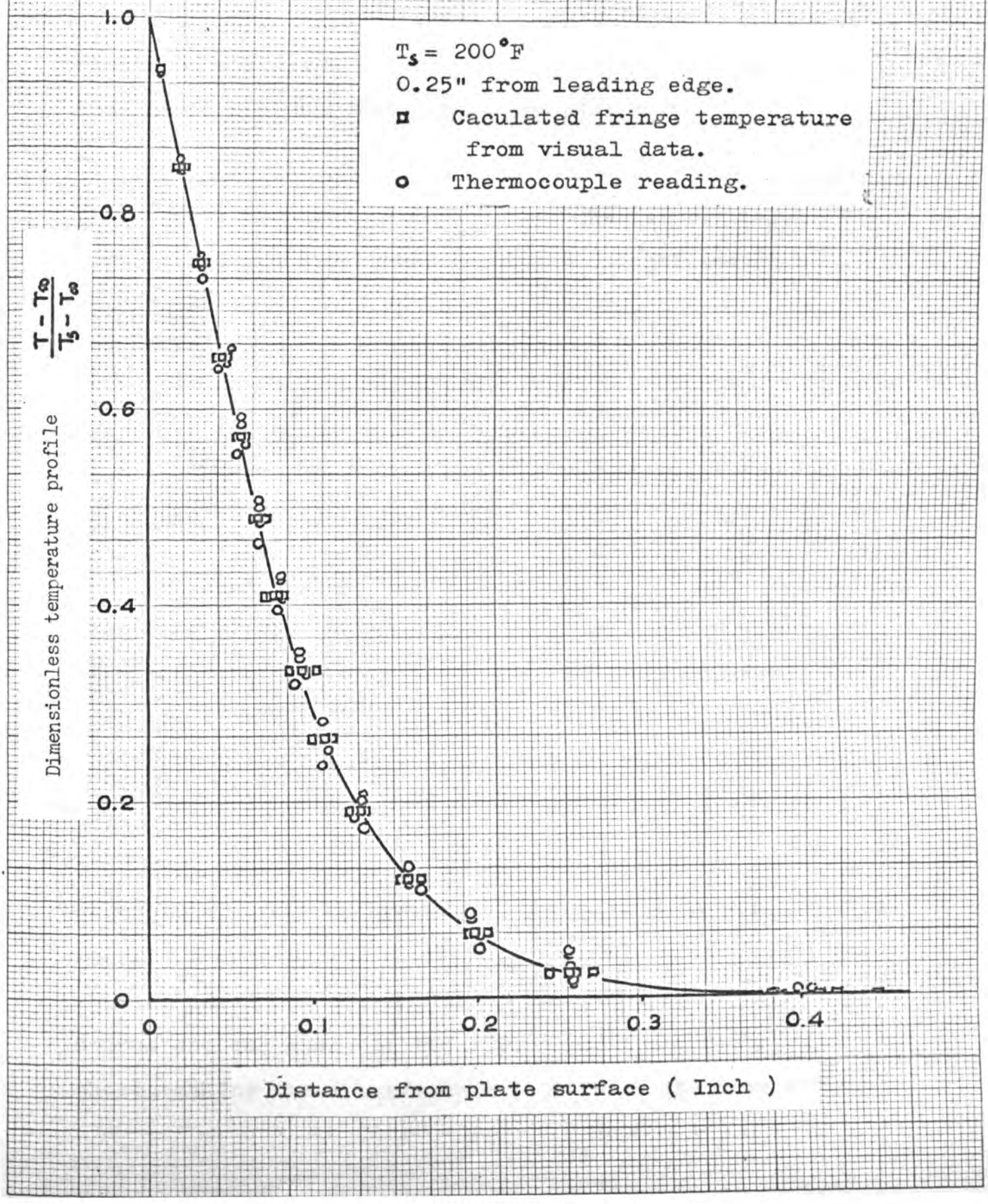

mental error.

Following the successful visual results, a series of photographs, of the interference patterns, was taken with test piece surface temperatures ranging from 120° F to 375° F.

For the flat plate, data were taken at points ranging from 0.0625 inch to 1.5 inches from the leading edge. The heated flat plate was held at many different angles to obtain different flow patterns. The angles were: (1) horizontal with the hot surface placed upward, (2) horizontal with the hot surface placed downward, (3) vertical, (4) 45 degrees with the hot surface upward, and (5) 45 degrees with the hot surface downward. A typical photograph for each case is shown in Fig. 14, 17, 18, 19, & 20.

Because of the many fluctuations in the boundary layer thickness of the horizontal wire, caused by turbulence in room air, the data were taken only in the temperature range from 150 F to 210 F. Positions of 90 degrees downward, horizontal, and 90 degrees upward were selected for taking data. Typical photographs are shown in Fig. 21.

Kodak Tri-X Pan film of ASA speed 400 was used for photographing the interference pattern through the telescope. A shutter speed of 1/2 second was used. This shutter speed was determined by the intensity of the light source and the speed of the film. For the purpose of photographing the interference pattern of the free convec-

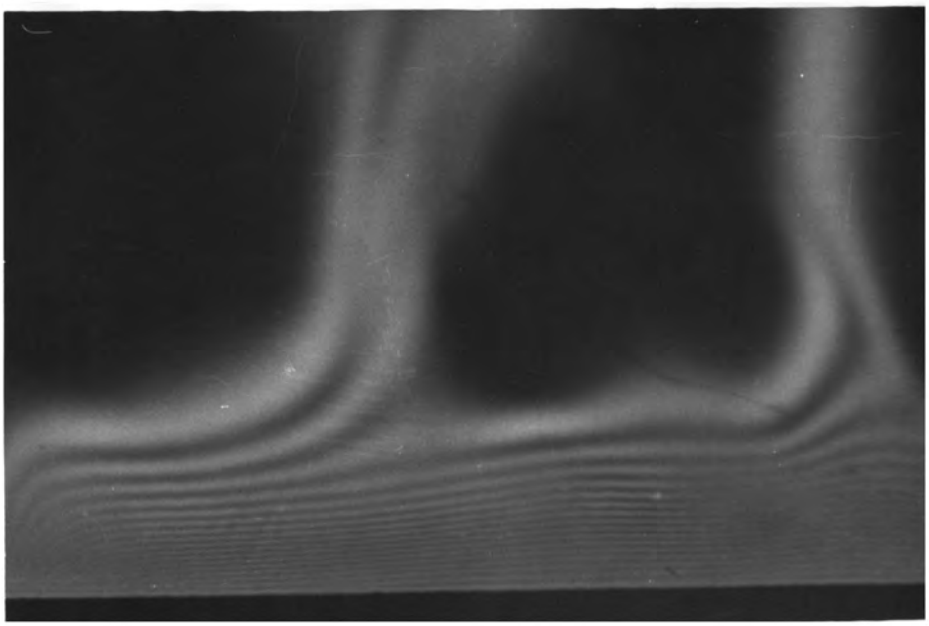

Fig. 17. Schlieren interferogram of heated horizontal plate with hot surface upward.

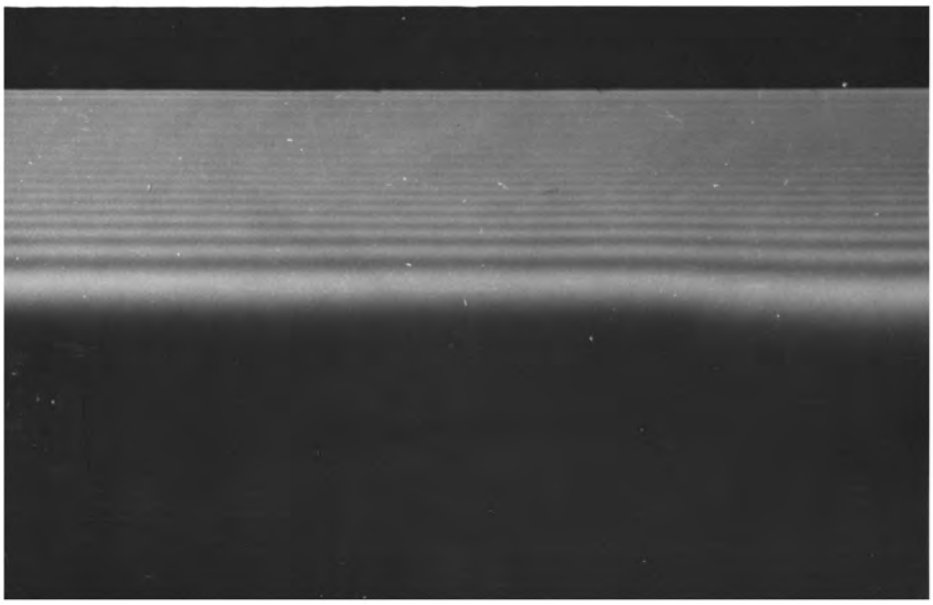

Fig. 18. Schlieren interferogram of heated horizontal plate with hot surface downward.

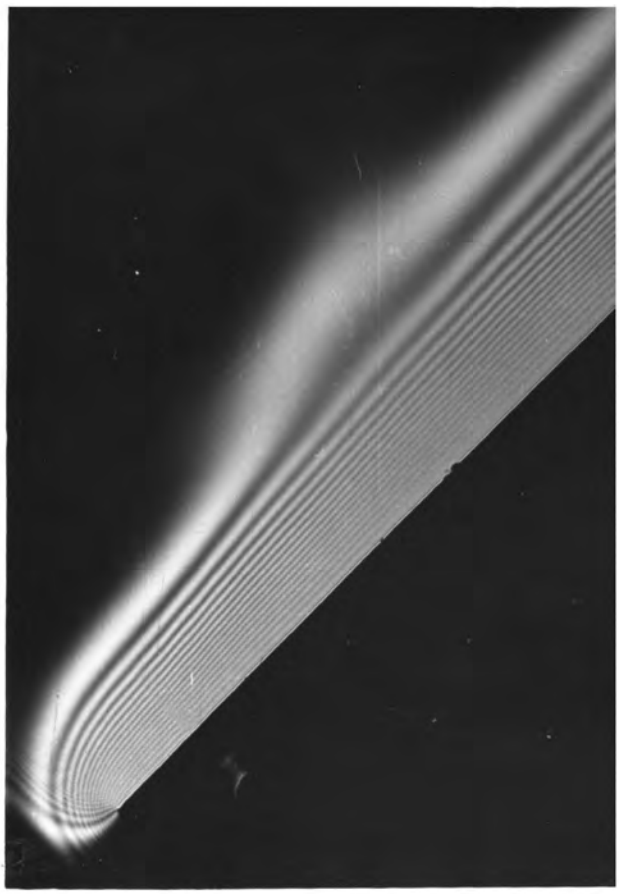

Fig. 19. Schlieren interferogram of heated flat plate held at 45 with hot surface upward.

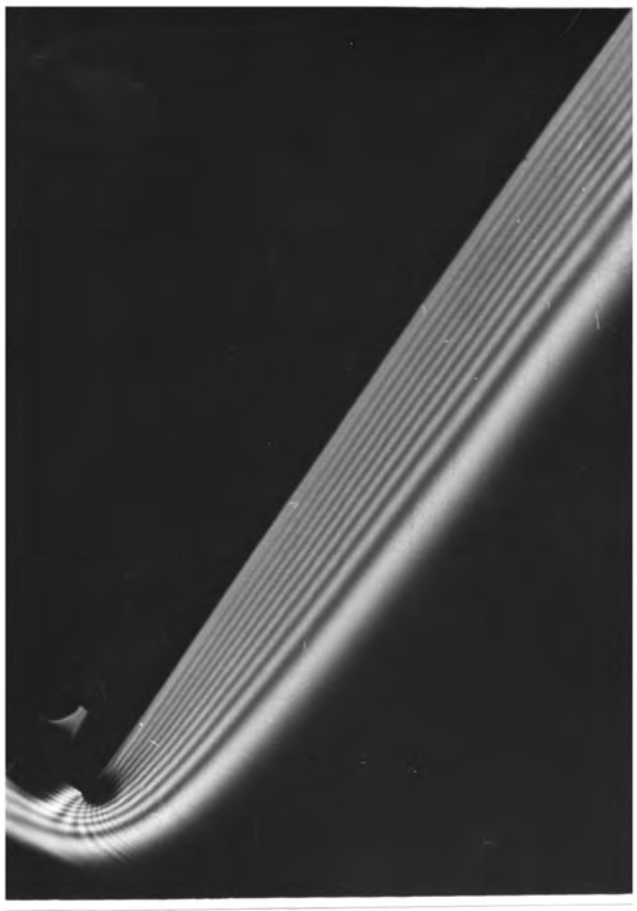

Fig. 20. Schlieren interferogram of heated flat plate held at 45 with hot surface downward.

Fig. 21. Schlieren interferogram of a horizontal heated wire 0.03" in diameter.

tive boundary laver in these experiments, this shutter speed was fast enough. The film was processed by a conventional method and it was read directly on a microfilm reader in the UMR library.

Interpretation of Interferograms:

Assume the following conditions: Two dimensional flow, a test piece 4 inches long, with negligible end effects, and monochromatic green light with a wavelength of 5300 Å. The corresponding Dale-Gladstone constant (K) is 3.637×10^{-3} cubic foot per pound mass. According to the Dale-Gladstone law, the relationship between the gas density (ρ_o) and the index of refraction (n_o) in the undisturbed field is

$$(1 + K\rho_o)L = n_o L,$$

where L is the length of the test piece. The same relationship holds true for the first maximum intensity line in the disturbed region, i.e.,

$$(1 + K\rho_1)L = n_1 L.$$

It is recognized that $n_o L$ is the optical path length in the undisturbed field and $n_1 L$ is the optical path length in the first maximum fringe. By the definition of interference, the difference in the optical path length between adjacent fringes is equal to one wavelength (λ). Therefore, we have the relation

$$(1 + K\rho_0) - (1 + K\rho_1) = n_0 L - n_1 L = \lambda .$$

Solving for ρ_1,

$$\rho_1 = \rho_0 - \frac{\lambda}{KL},$$

and the difference of density between the adjacent fringes is

$$\Delta\rho = (\rho_m - \rho_{m+1}) = \frac{\lambda}{KL},$$

a constant, where m is any one fringe.

In the experiments, the atmospheric pressure was 29 inch Hg., and the temperature of the undisturbed field (T_∞) was 85°F. By the ideal gas law, the density of the undisturbed field was 0.0706 pound mass per cubic foot. The difference in the density of the air between adjacent fringes was 1.434×10^{-3} pound mass per cubic foot.

The temperature of each fringe (T) listed in Table II was calculated using the ideal gas law. Because of the low temperature and pressure, the deviation of the results calculated from the ideal gas law was negligible in comparison to the measuring errors.

For the heated flat plate, the temperature distribution in the boundary layer was plotted as a dimensionless temperature profile ($\frac{T-T_\infty}{T_s-T_\infty}$) versus distance from the heated flat plate surface. The data obtained for different plate surface temperatures (T_s), at the same distance from the leading edge with like plate inclination were plotted

TABLE II. FRINGE TEMPERATURE (T)

Fringe No.	T	$T - T_\infty$*
0	85° F	0
1	96.5	11.5
2	108.5	23.5
3	120.5	36.0
4	133.5	49.0
5	147.0	52.5
6	161.0	66.5
7	175.5	81.0
8	190.5	96.0
9	206.5	122.0
10	223.5	139.0
11	241.5	157.0
12	260.5	176.0
13	280.5	196.0
14	301.5	217.0
15	323.5	239.5
16	347.5	263.5
17	373.0	289.0
18	400.0	316.0
19	428.5	344.5
20	458.5	374.5

*The temperature difference ($T - T_\infty$) versus number of fringes were plotted on Fig. 22.

Fig. 22 . Theoretical temperature difference of interference fringes.

T_{∞} = 85°F
P_{atm} = 29.0" Hg.
λ = 5300 Å
K_{G-D} = 3.637×10^{-3} cu.ft./lb
L = 4"

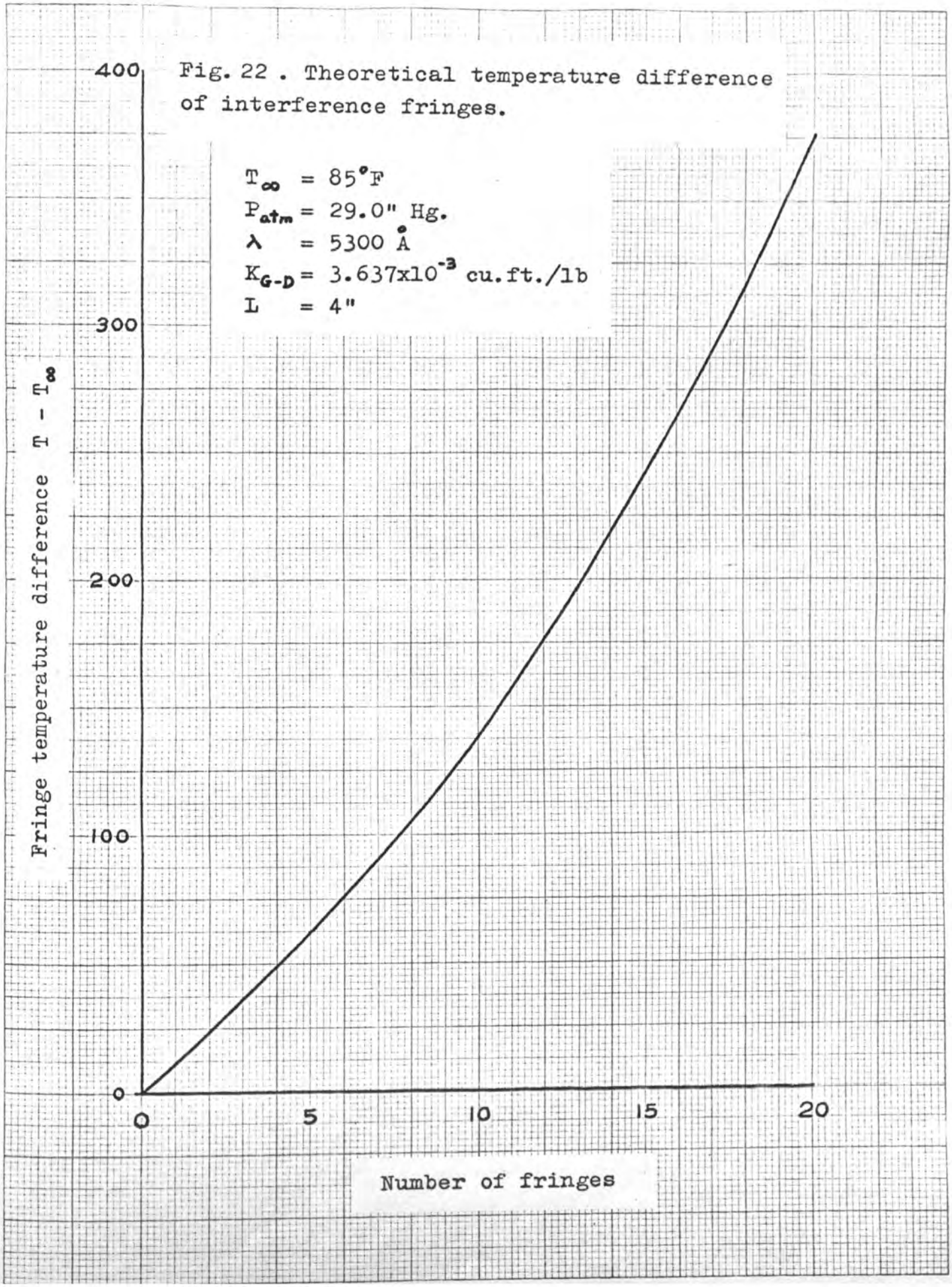

on one graph. These graphical results are shown in Fig. 23-33. The curves for different distances along the leading edge at like plate inclinations were plotted on one graph by modifving the abscissa. These curves are shown in Fig. 34, 35, & 36. The curves in Fig. 23, 24, 34, 35, 36 were combined in one figure as shown in Fig. 37.

For the heated horizontal wire, the temperature distribution in the boundary layer was plotted as a dimensionless temperature profile ($\frac{T - T_\infty}{T_s - T_\infty}$) versus the radial distance from the heated wire surface. The data obtained for different wire surface temperatures were plotted on one graph as shown in Fig. 38.

Fig. 23 . Photographic results of temperature distribution in free convective thermal boundary layer of heated horizontal plate with hot surface upward. Data read at center line. T = 85°F T = 297°F

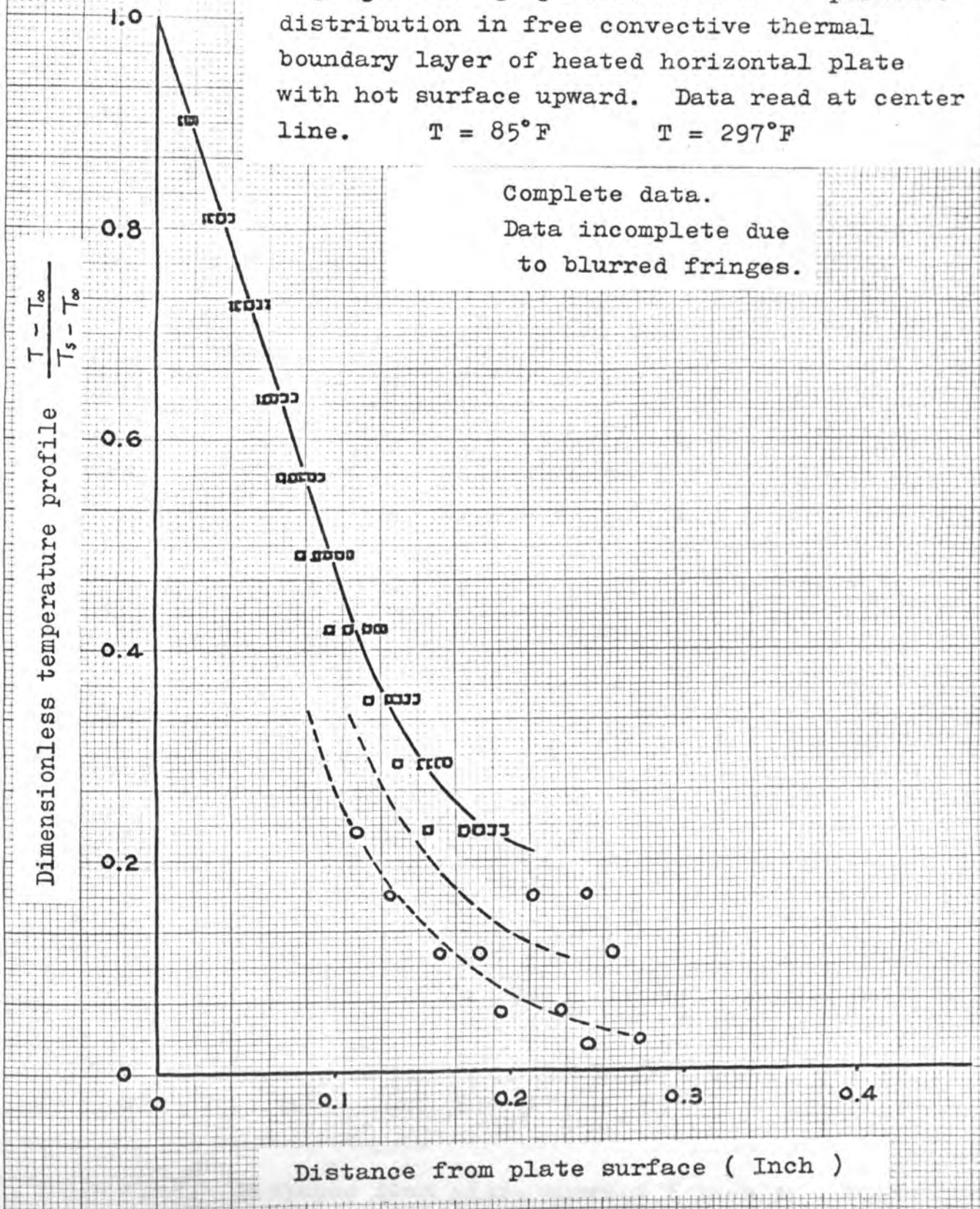

Fig. 24 . Photographic results of temperature distribution in free convective thermal boundary layer of heated horizontal plate with hot surface downward. Data read at center line. $T_\infty = 85°F$

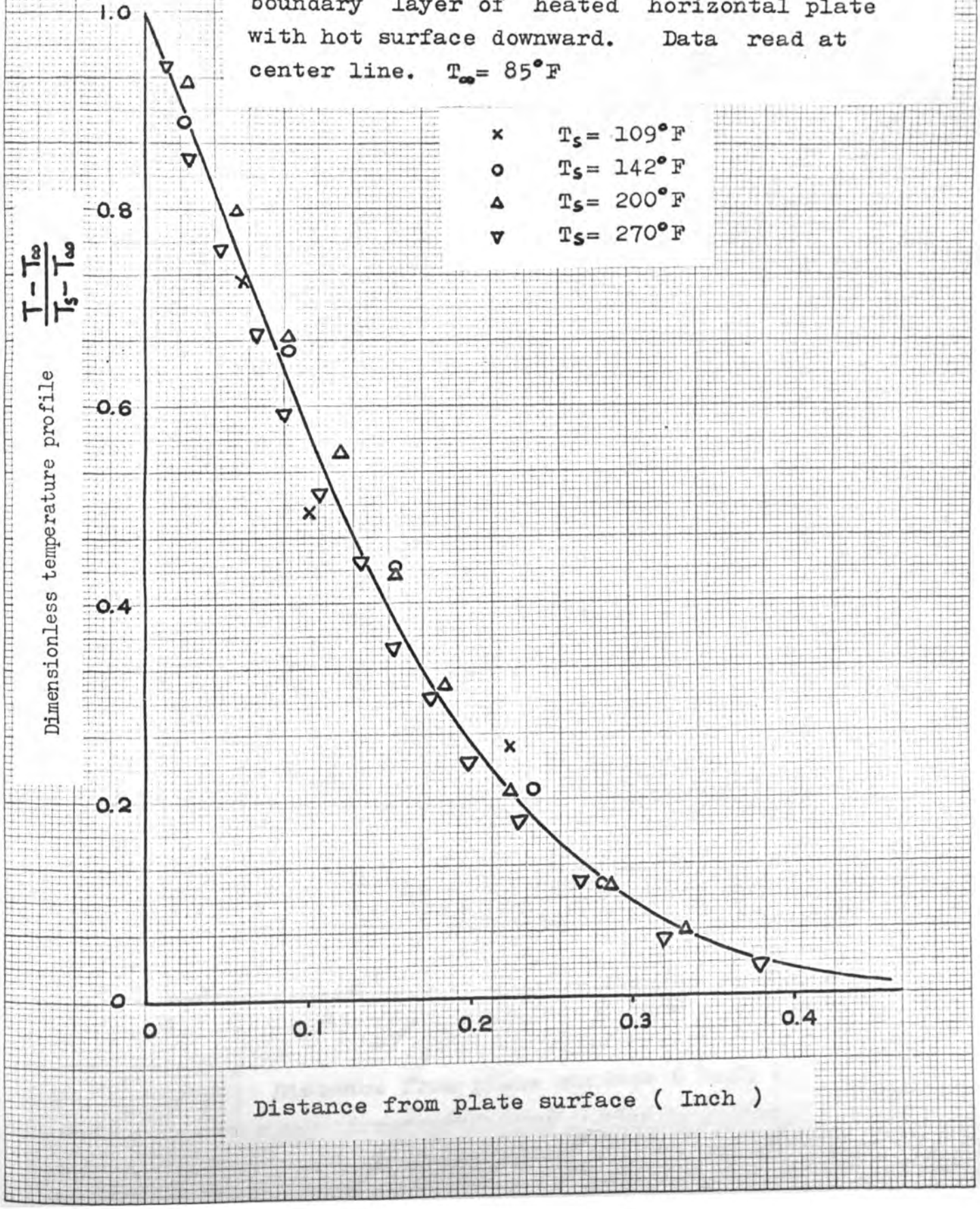

Fig. 25. Photographic results of temperature distribution in free convective thermal boundary layer of heated vertical plate at the point 0.0625" from leading edge. $T_\infty = 85°F$

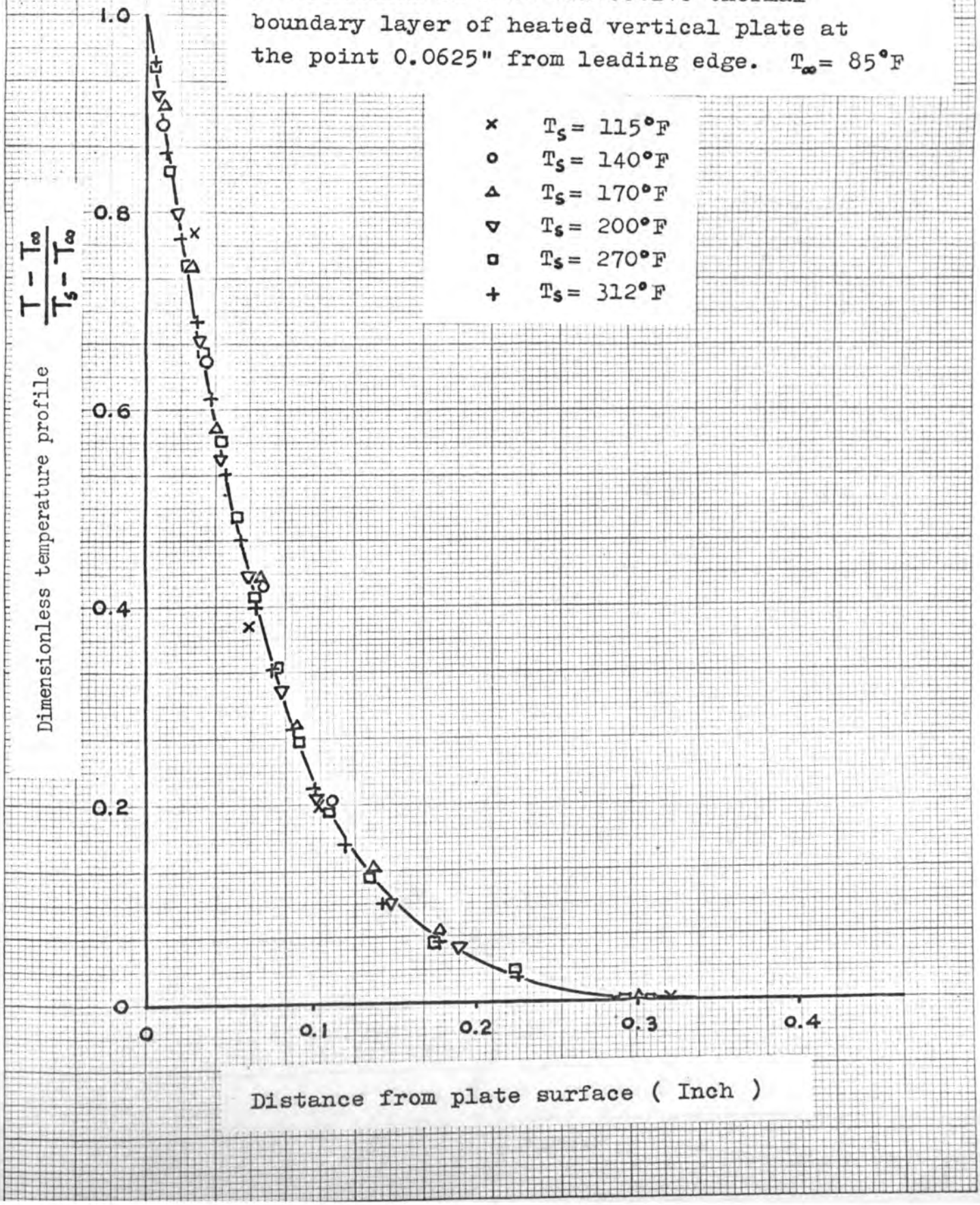

Fig. 26. Photographic results of temperature distribution in free convective thermal boundary layer of heated vertical plate at the point 0.25" from leading edge. $T_\infty = 85°F$

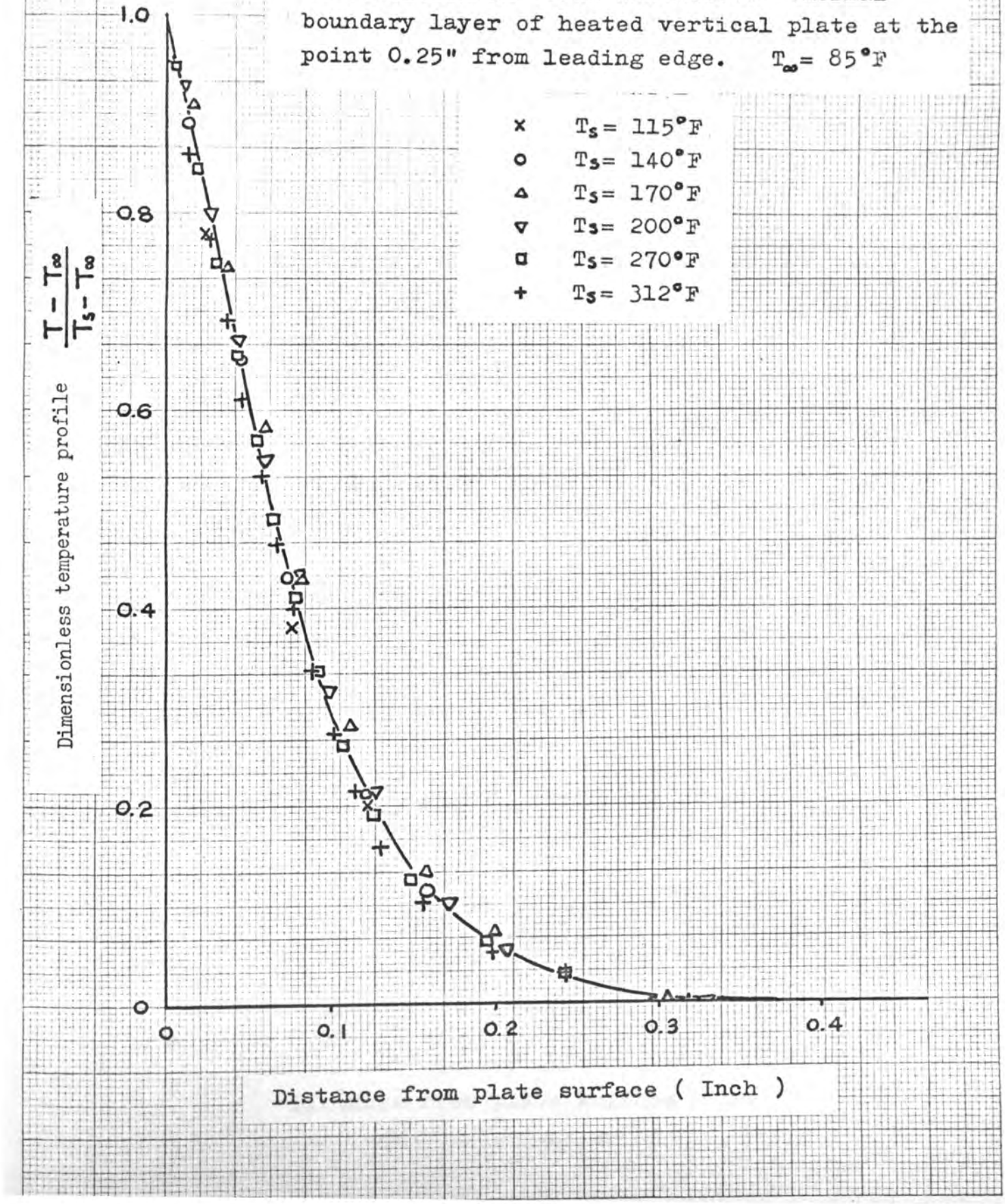

Fig. 27. Photographic results of temperature distribution in free convective thermal boundary layer of heated vertical plate at the point 1.50" from leading edge. $T_\infty = 85°F$

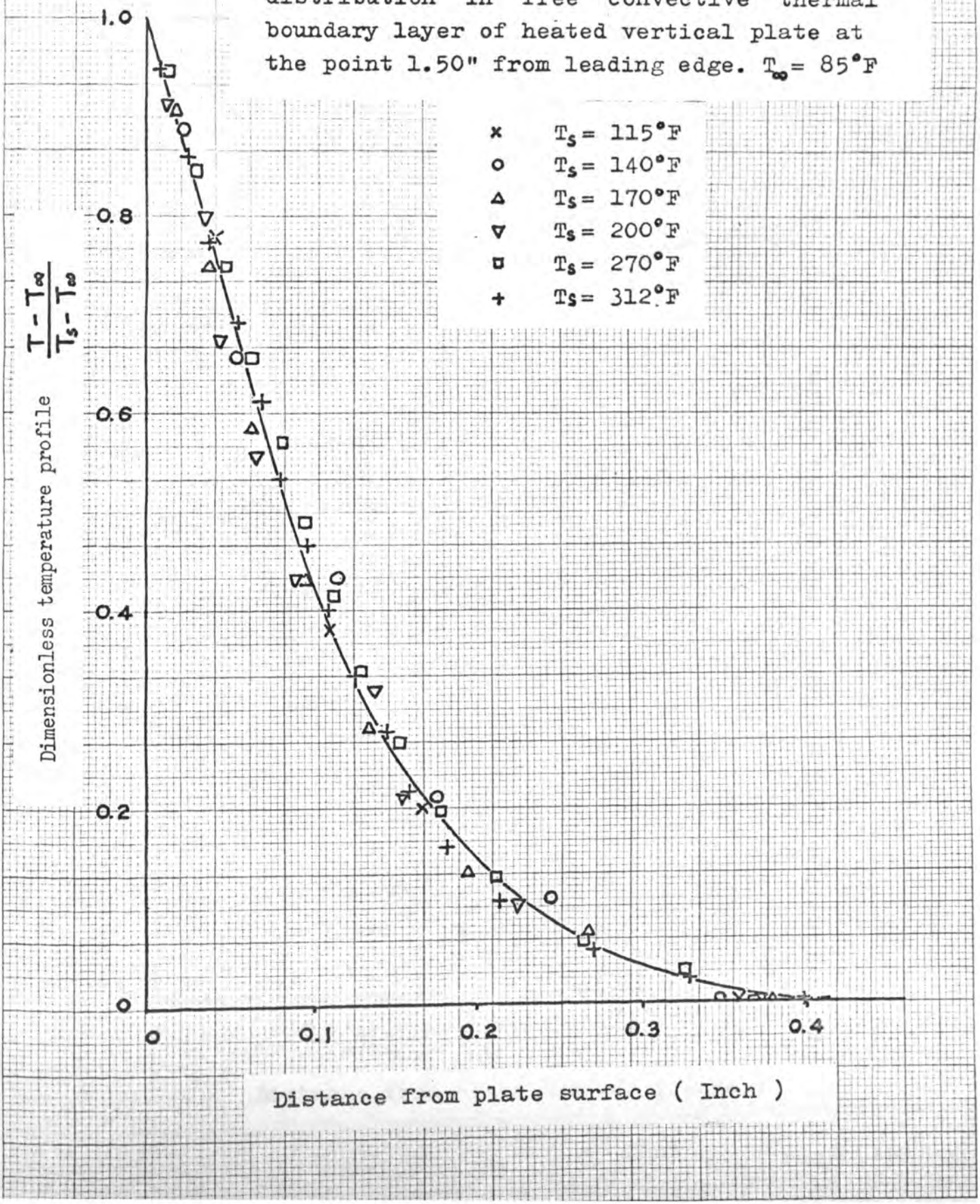

Fig. 28 . Photographic results of temperature distribution in free convective thermal boundary layer of heated plate 45° upward at point 0.0625" from leading edge. T_∞ = 85°F

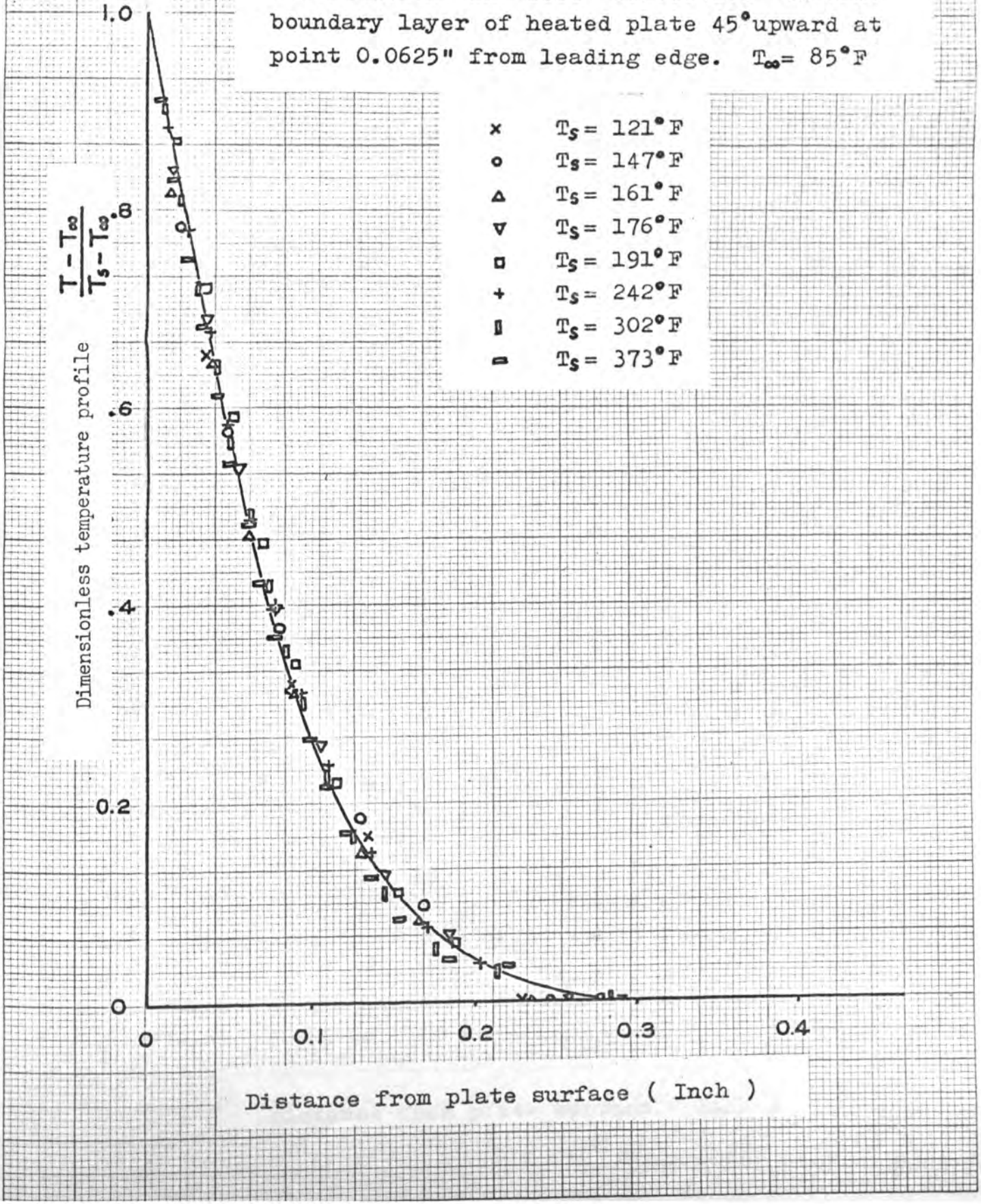

Fig. 29. Photographic results of temperature distribution in free convective thermal boundary layer of heated plate 45°upward at point 0.25" from leading edge. T_∞= 85°F

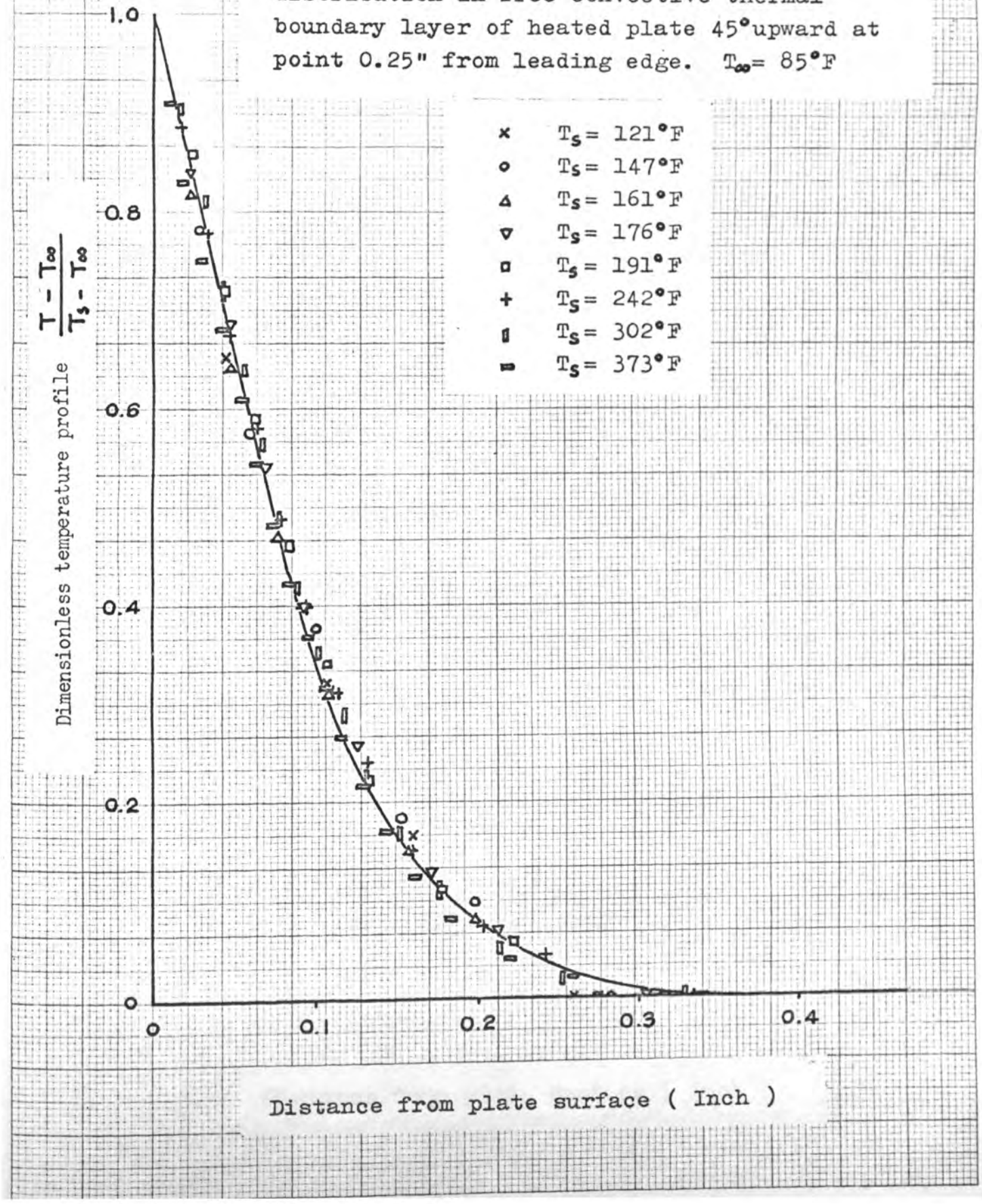

Fig. 30. Photographic results of temperature distribution in free convective thermal boundary layer of heated plate 45° upward at the point 1.50" from leading edge. T_∞= 85°F

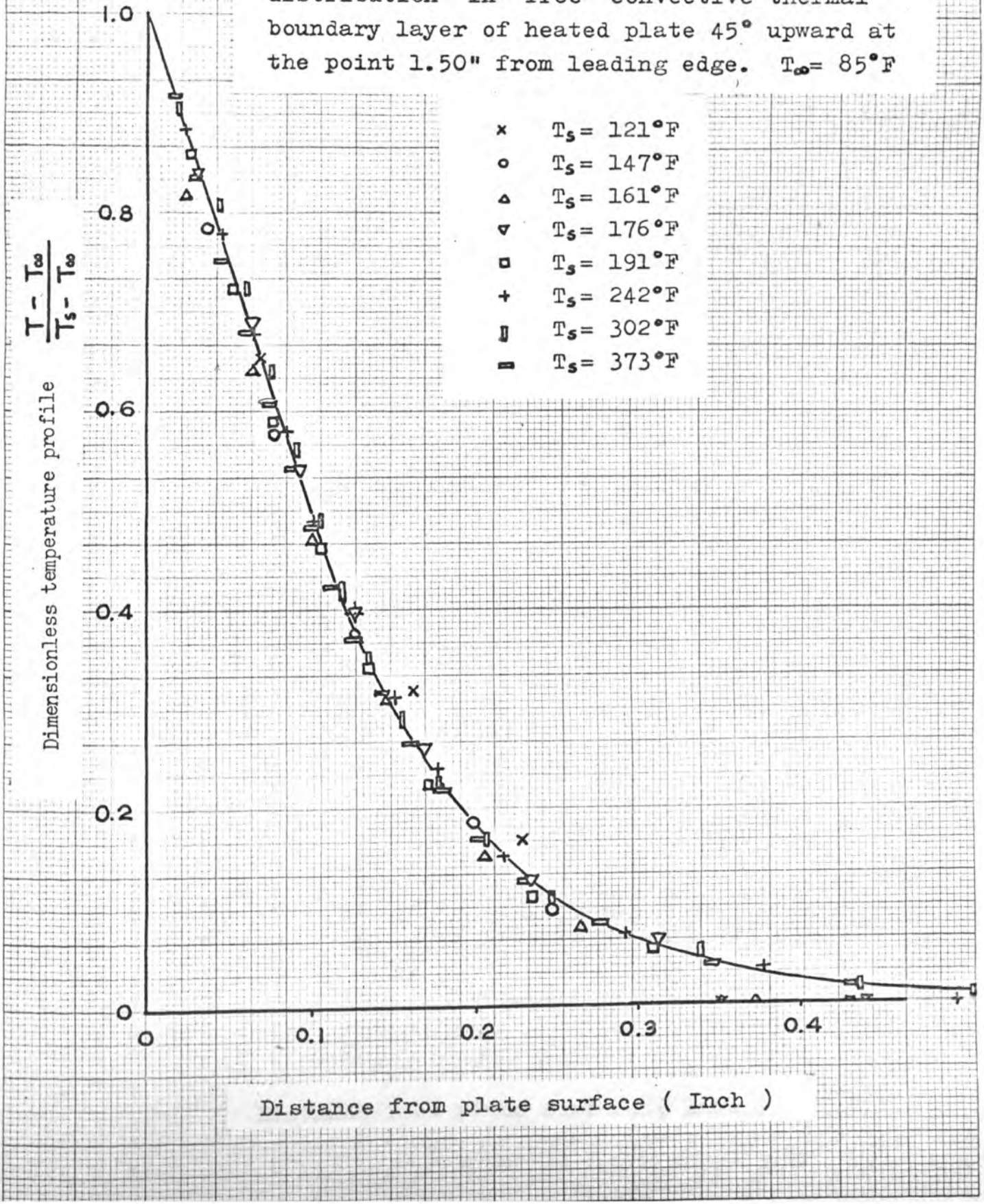

Fig. 31. Photographic results of temperature distribution in free convective thermal boundary layer of heated plate 45°downward at the point 0.0625" from leading edge. T_∞= 85°F

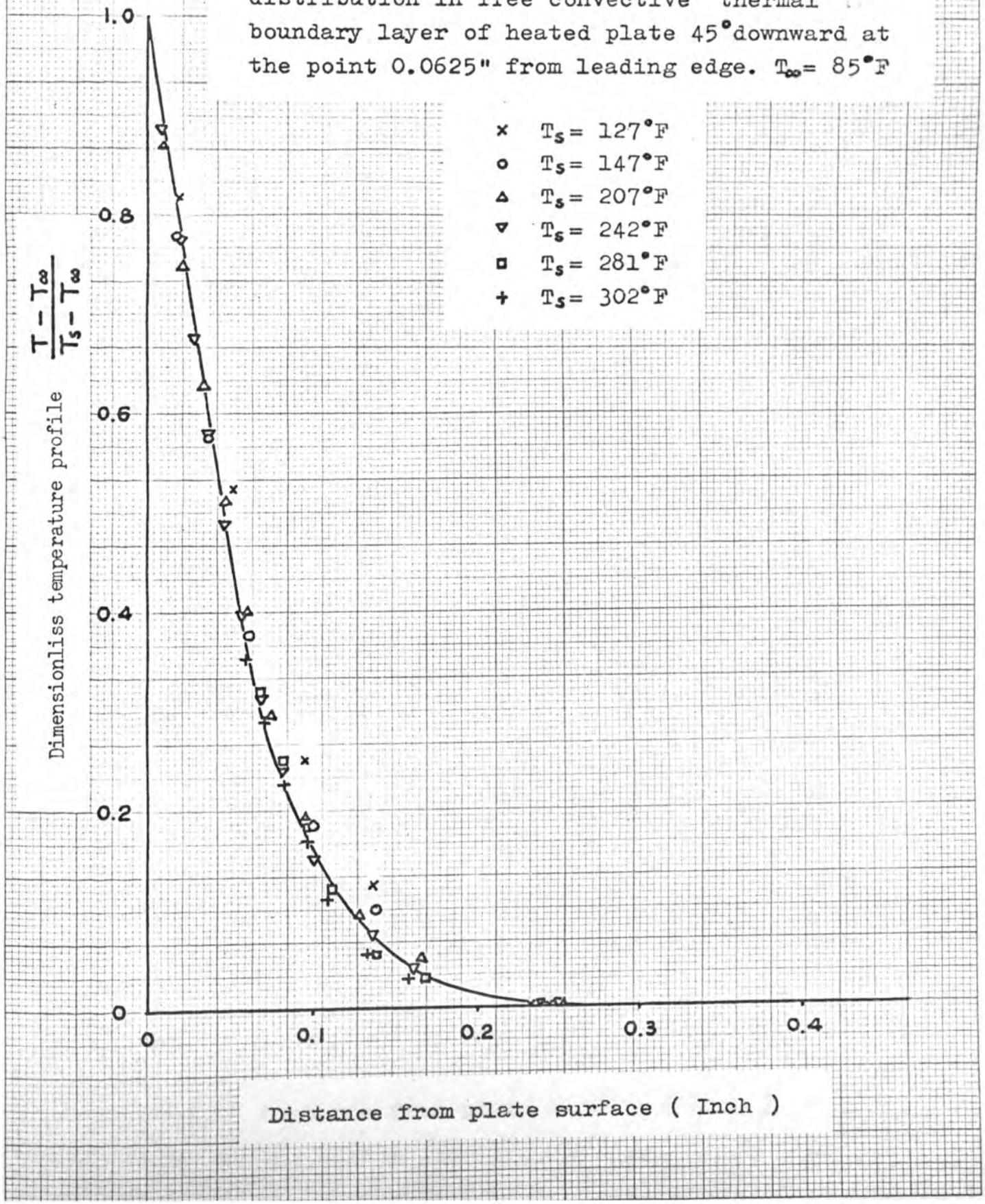

Fig. 32. Photographic results of temperature distribution in free convective thermal boundary layer of heated plate 45° downward at the point 0.25" from leading edge. T_∞ = 85°F

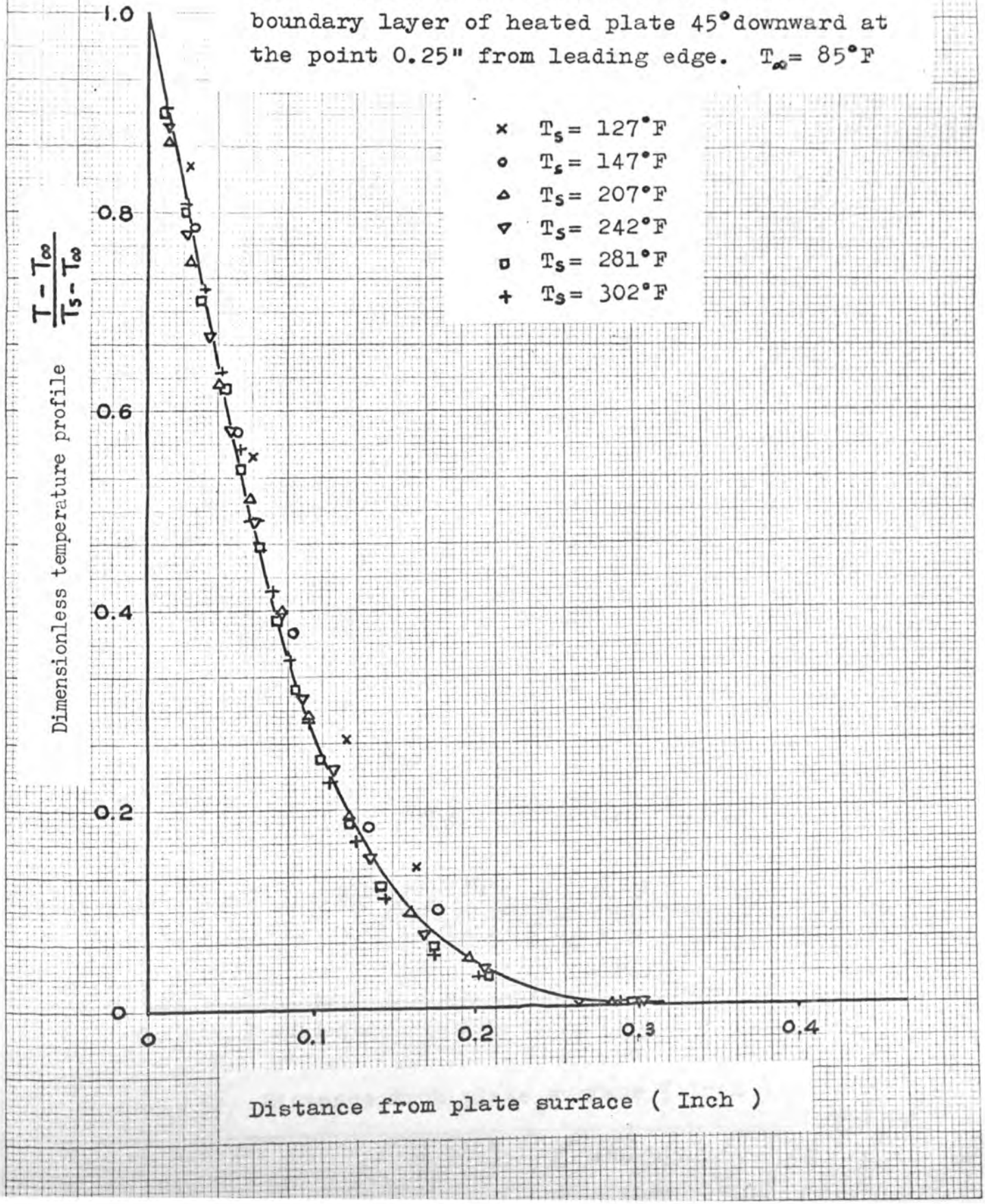

Fig. 33. Photographic results of temperature distribution in free convective thermal boundary layer of heated plate 45° downward at the point 1.50" from leading edge. T_∞ = 85°F

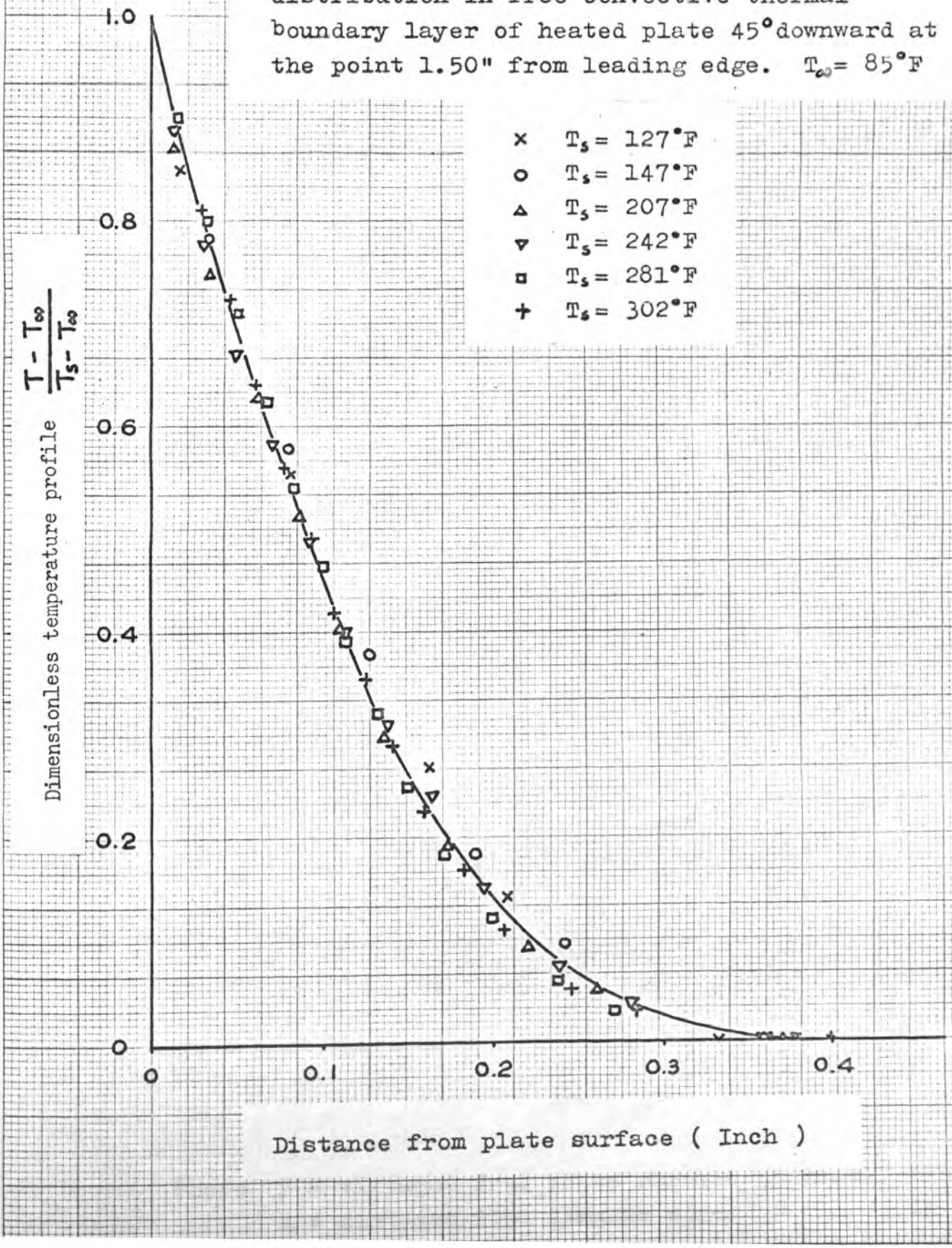

Fig. 34. Generalized temperature distribution curve for free convective thermal boundary layer of heated vertical plate.

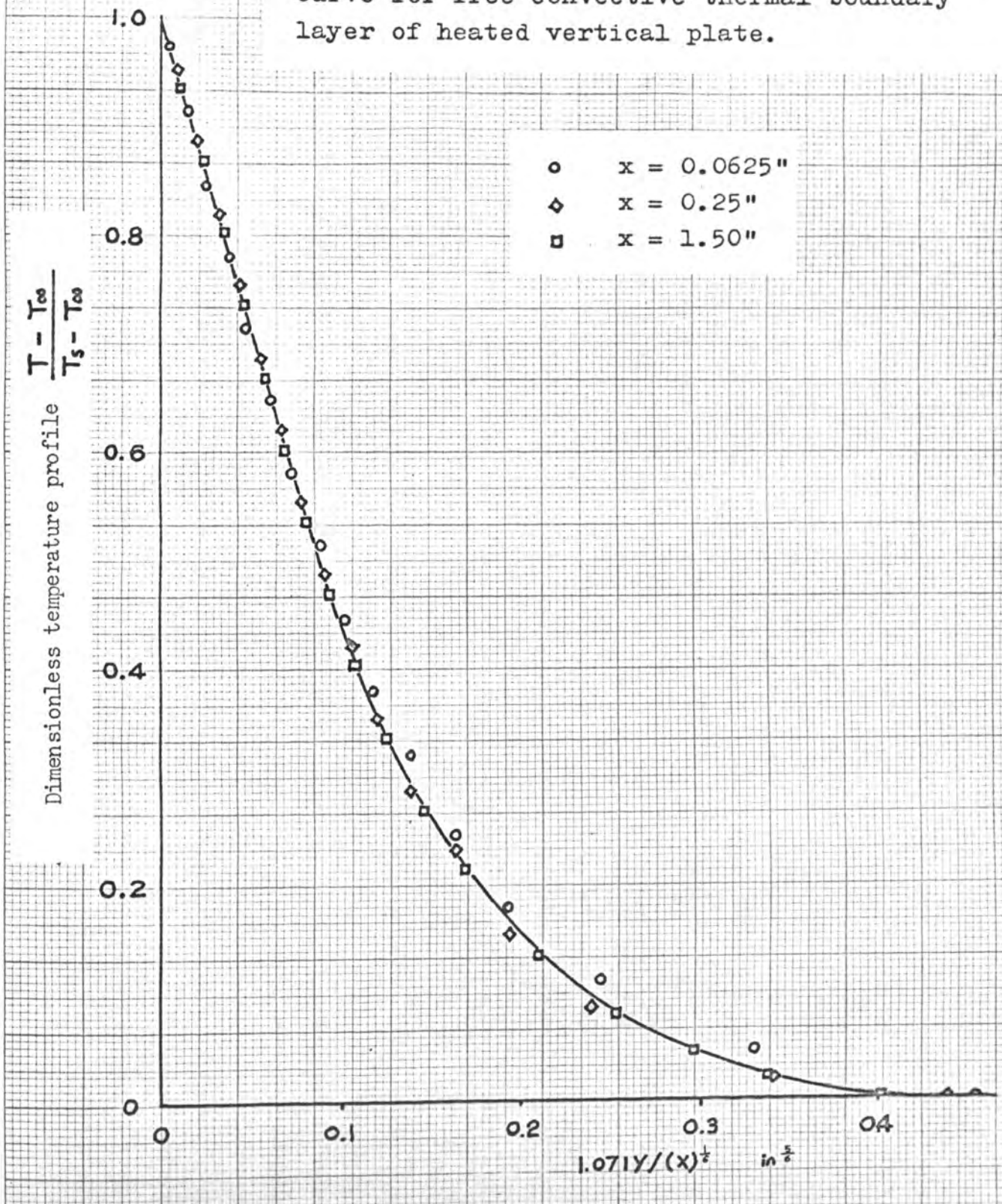

Where y = distance from plate surface in inch.
x = distance from leading edge.

Fig. 35. Generalized temperature distribution curve for free convective thermal boundary layer of heated plate with hot surface upward of 45° inclination.

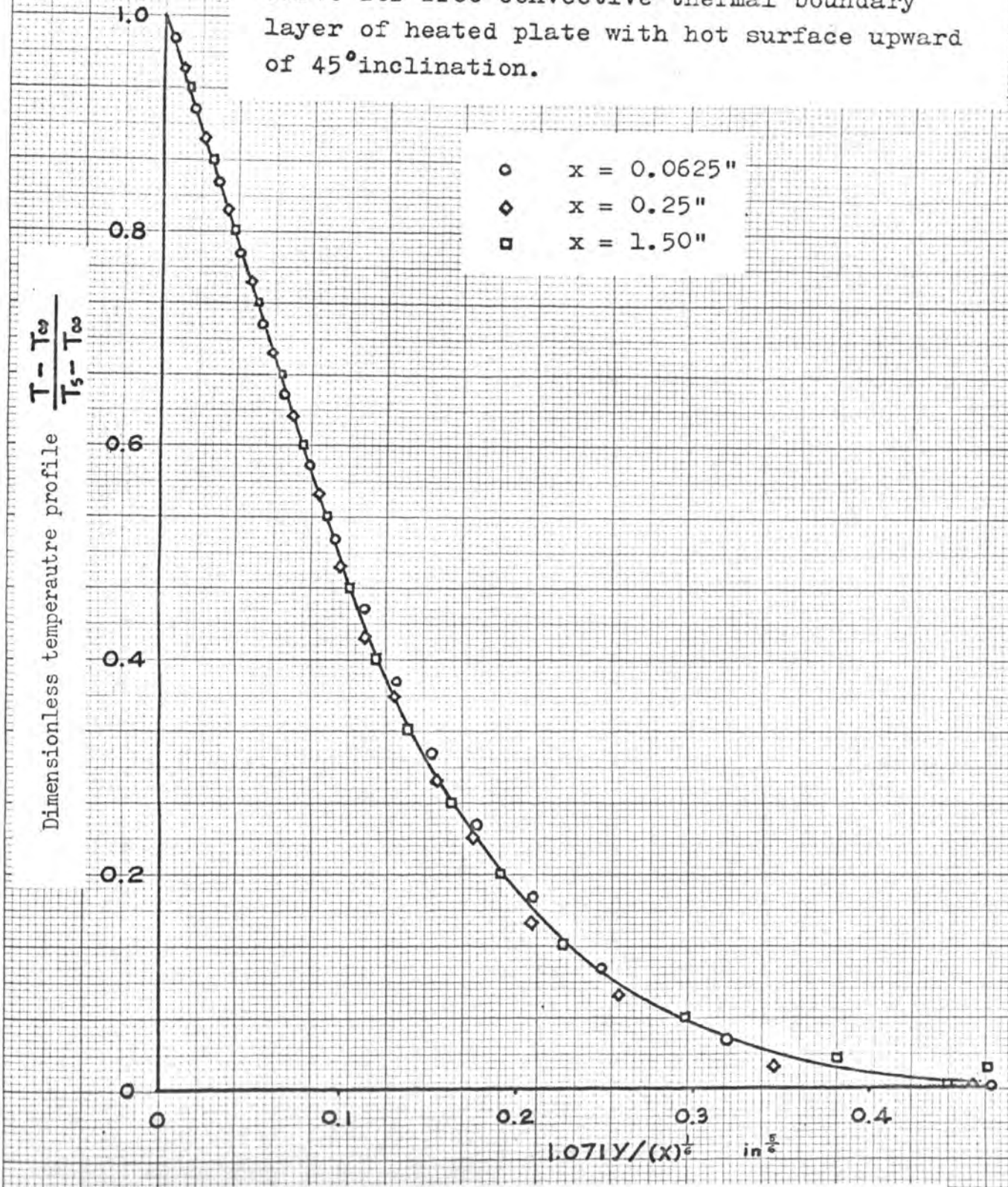

Where y = distance from plate surface in inch.
x = distance from leading edge.

Fig. 36. Generalized temperature distribution curve for free convective thermal boundary layer of heated plate with hot surface downward of 45° inclination.

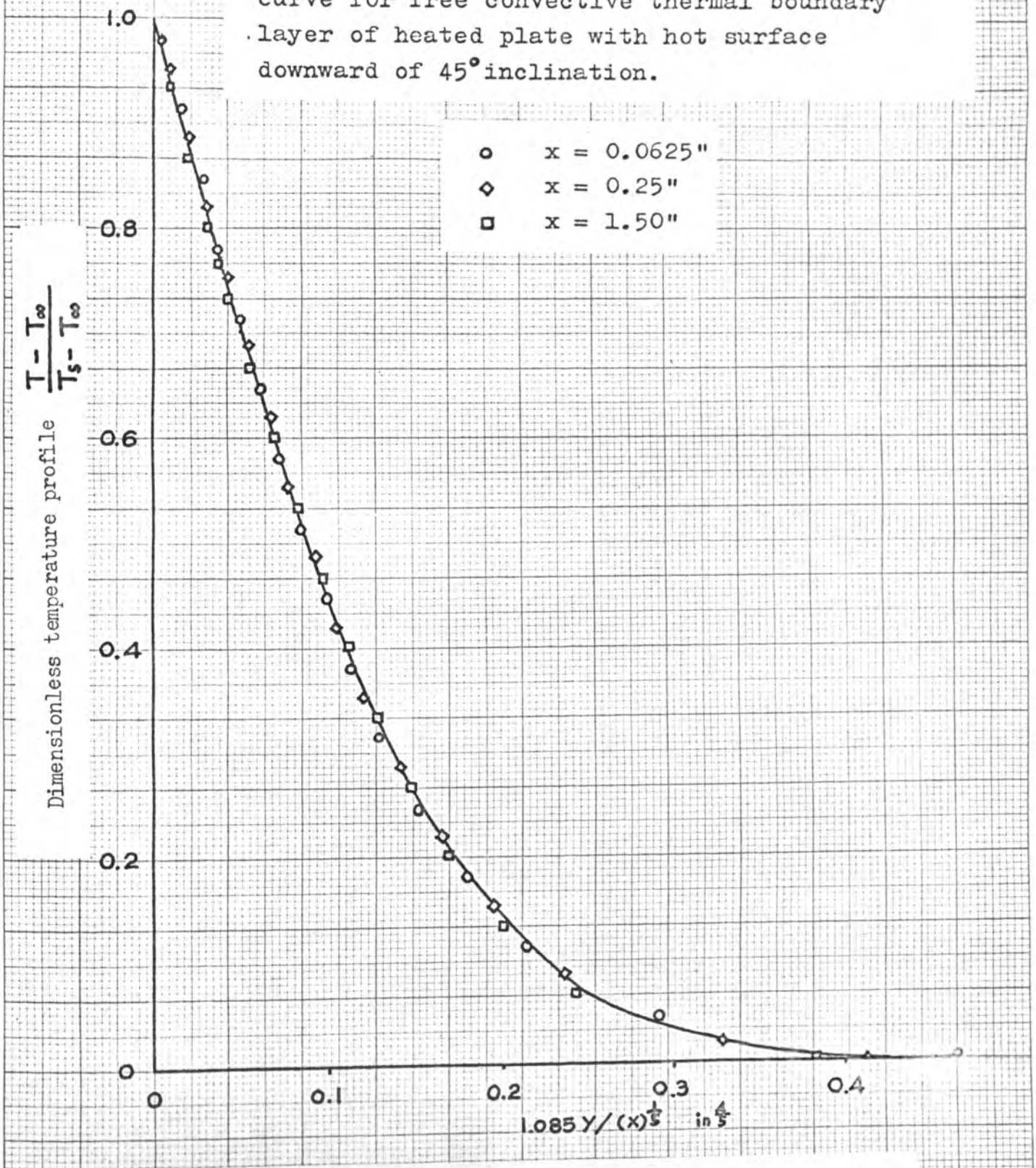

Where y = distance from plate surface in inch.
x = distance from leading edge.

Fig. 37. Temperature distribution of heated plate in free convection.

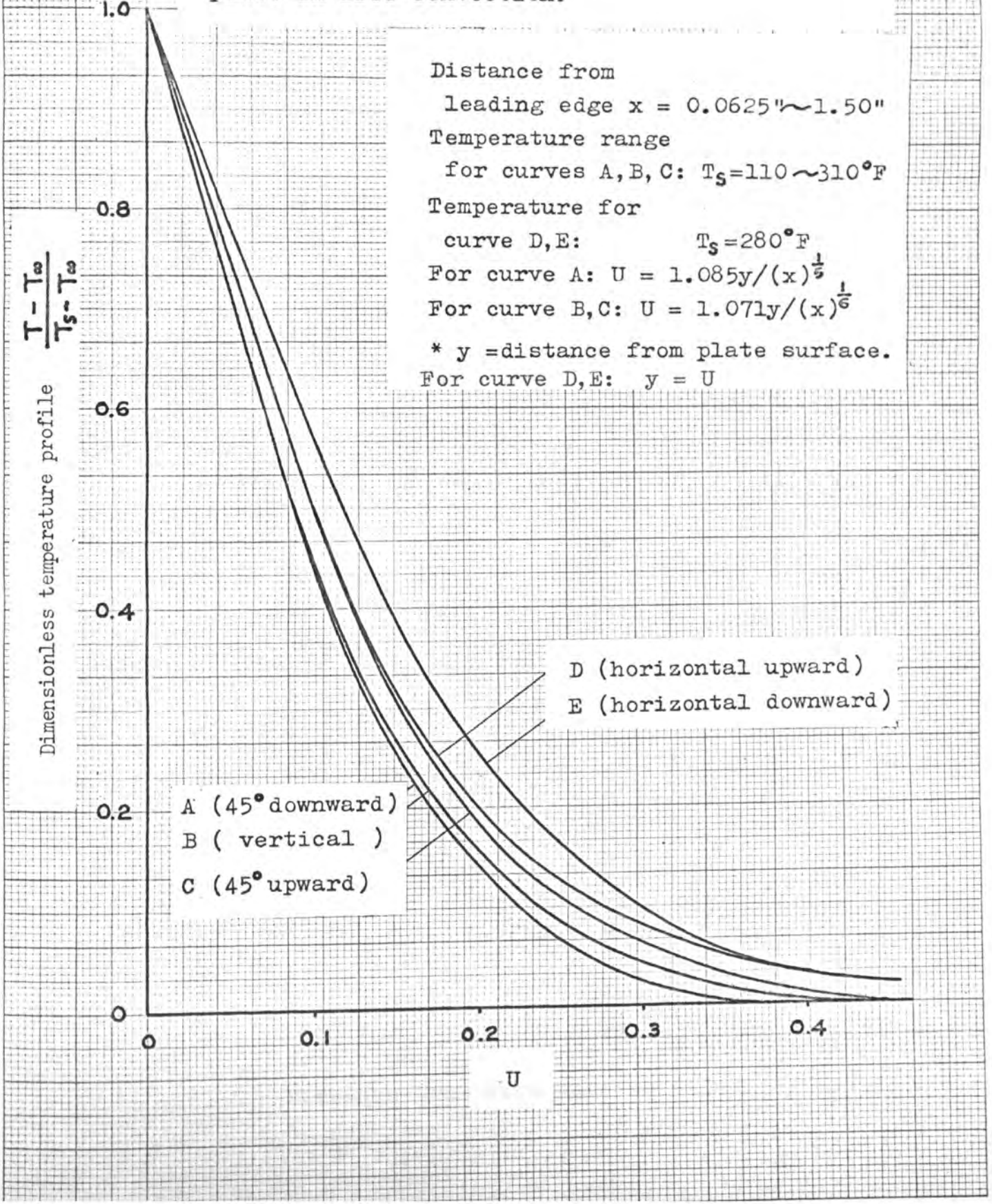

Fig. 38. Temperature distribution around a horizontal heated wire 0.03" in diameter.

Temperature range: T_s = 150~210°F
Curve A : 90° downward
Curve B : Horizontal
Curve C : 90° upward

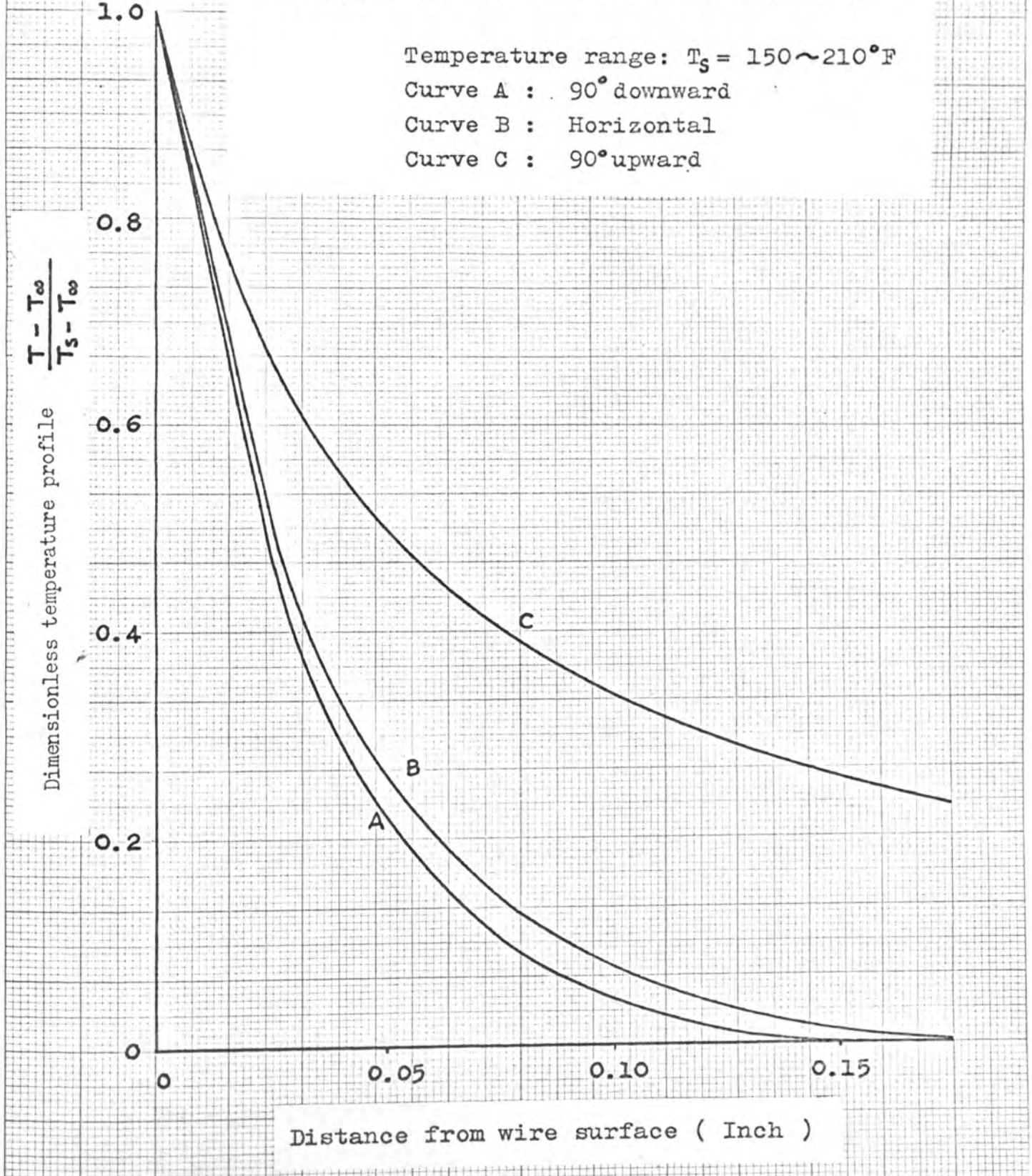

IV. DISCUSSION OF RESULTS

The apparatus as designed, constructed, and used in these experiments, performed favorably in the measurement of the temperature distribution in the thermal boundary layer of free convection.

Difficulties that limited the temperature measurement range of this apparatus were the fluctuation of the boundary layer thickness and the test piece end effects. The higher the test piece temperature, the greater were the end boundary layer effects, and these effects usually blurred the interference fringes. Therefore, the problem could no longer be treated as two dimensional. For better experimental results at higher temperature it is recommended that a pair of glass windows be used to make the test section two dimensional. This would also eliminate the end effects. The glass windows should be made of high quality optical glass.

The experiments made at low temperatures with $T_s - T_\infty$ ranging from 25° to 310° F. Consistent results were obtained, except for the data obtained near the edge of the boundary where the undisturbed field air turbulence had a tendency to affect the laminar flow. Otherwise, the results in the laminar flow region seemed to be reasonable.

The experimental results for the flat plate when

placed at different angles were surprisingly stable except for the horizontal position with the hot surface placed upward. Although the investigation was limited between 0.0625 inch to 1.5 inches from leading edge, a longer and wider test piece could be used with suitable modifications to the test piece holder.

The horizontal plate with the hot surface facing upward was the most difficult to observe, since its inherent unstable convective currents make the temperature in the outer parts of the boundary layer fluctuate wildly. This temperature fluctuation happened only for a temperature difference of approximately 100 F between the undisturbed region and several fringe depths at high surface temperature. The corona shaped currents flowed upward and with lateral motion from the edges of the boundary layer as shown in Fig. 12 & 17. Therefore, the temperature distribution in this region was very difficult to determine from the interferograms, because they do not show depth. However, Schlieren interferometry is still an excellent method for qualitative studies of horizontal surfaces facing upward.

The horizontal plate with the hot surface facing downward also possesses inherent unstable convective currents because the flow velocities were low with the plate in certain positions. The strong upward flow current at the edge or the ends of the plate usually blurred the inter-

ference fringes. (See Fig. 18) This difficulty could be overcome by glass windows at the ends of the test piece.

The experiments involving the horizontal wire were much more difficult to conduct than for the flat plate, because the convective currents were much weaker than those for the plate, and the wire temperatures were affected more by the surrounding air disturbances. In addition, undesired interferences due to the geometry of the cut-off edge and the curved temperature field made the interpretation of the results difficult. (Refer to Fig. 21)

For horizontal wires, cylinders, or other irregular two dimensional test pieces, it is recommended that a narrow ring shaped light source be used instead of a line source. The diameter of the ring should be 2 to 3 mm, and the width should be less than 0.1 mm to fit the present system. The knife-edge should be replaced by a circular opaque disc. The ring and the disc can best be made by photographic technique. With this modification, it would be possible to eliminate the undesired interferences.

The author has an idea of making a monochromatic ring-shaped light source by using a simple convex lens made of high dispersive glass. For a spherical aberration corrected simple lens, light of different colors could be focused at different points if the lens is illuminated by parallel light or a point source. If a small ring-shaped aperture

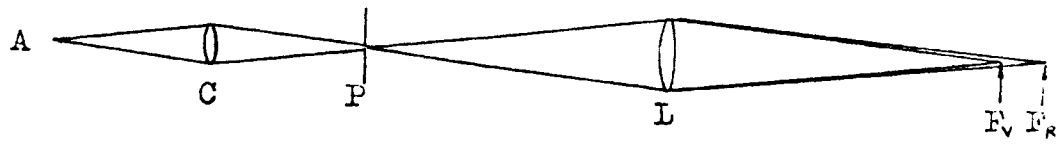

(a)

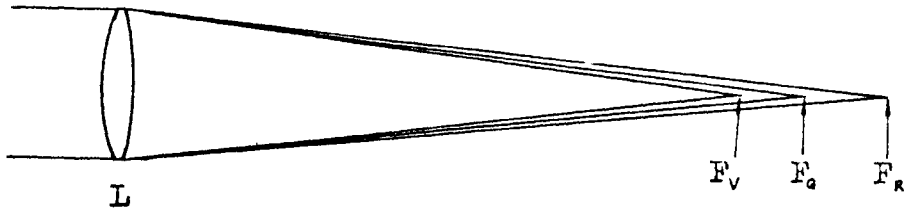

(b)

(c)

(d)

Figure 39 . (a) Optical layout of two dimensional monochromatic and color lgith source. (b) The dispersion of simple lens. (c) Ring shape light source, and(d) Pin-hole light source.

was located at the focus of the lens, it would be possible to obtain a monochromatic ring source. (Refer to Fig. 39)

For high speed photography the apparatus used in this thesis should be modified by using a high intensity light source such as an arc lamp.

In general, Schlieren interferometry is quantitatively excellent for two dimensional investigations and qualitatively for three dimensional use. Since it is an optical method, the flow path to be investigated should be defined by transparent flat windows of high quality optical glass. This requirement limits the application of this method.

The recommendations indicated are not absolutely necessary, but are offered as means of further applications of Schlieren interferometry, with the hope that a better insight may be derived in convective studies. With the technique developed in this investigation, the free convective boundary layer may be inspected very effectively.

V. BIBLIOGRAPHY

1. Hawkins, G. A., (1950), Elements of Heat Transfer, p. 112.

2. Kreith, F., (1958), Principle of Heat Transfer, International Textbook, Scranton, p. 241-2.

3. Shapiro, A. H., (1953), The Dynamics and Thermodynamics of Compressible Fluid Flow, Ronald, New York, p. 59-60.

4. Barnes, N. F. & Bellinger, S. L., (1945), Schlieren and Shadowgraph Equipment for Air Flow Analysis, Journal of the Optical Society of America, V 35 No 8., p. 497-507.

5. Stong, C. L., (1964), How to Photograph Air Current in Color, Scientific American, Feb. 1964.

6. Temple, E. B., (1956), Quantitative Measurement of Gas Density by Means of Light Interference in a Schlieren System, Journal of the Optical Society of America, V 47 No 1., p. 91-100.

7. NAVORD Report 1488 (Vol 6, Sec 18), Optical Method, p. 534.

VI. APPENDIX I

PROCEDURES FOR USING THE INSTRUMENT

1) Light Source System: (Refer to Fig. 4)

First, adjust the position of the condenser along its optical axis to form a sharp image of the light bulb filament at the plane of the first narrow slit (S_1) and then adjust the position of the image of the filament to the center of the slit by turning the three screws at the bulb socket base. The distance between the first slit and the collimator is fixed at 178 mm, exactly one focal length of the collimator. This can be checked by aiming the collimator at a long distance subject, such as a street light or the rising moon. Then adjust the collimator to form a sharp image of the street light or moon on the plane of slit S_1. Remove the prism and turn the system to place every optical part on one common optical axis. This can be easily seen if the image of the first slit falls on the second slit S_2 which was centered previously. The next step is to adjust the focus of the telescope objective lens (L_2) to form a clear image of the first slit on the plane of second slit (S_2). Move the movable arm of the light source system to about 30 degree and insert the prism into the system. Then adjust the movable arm to make the spectrum fall just on the second slit (S_2). The prism should be placed symmetrically to both incidental light and refracting light.

2) Diagonal Mirror D_1 & D_2: (Refer to Fig. 4)

Put the complete light source system in place and adjust the distance from the second slit (S_2) to the first concave mirror (M_1) to exactly one focal length (45 inches). Apply the light source, and place a 7 by 7 inches white cardboard with a 4 inch circle at center in front of the first mirror (M_1). This shows if the light from the second slit (S_2) impinges on the first concave mirror (M_1); if not, adjust the diagonal mirrors (D_1 & D_2) to make the light spot exactly coincide with the 4 inch circle with approximately a one half inch margin.

3) First Concave Mirror M_1: (Refer to Fig. 4)

The adjustment of the first concave mirror can be achieved by placing the same white cardboard in front of the second concave mirror (M_2) to see if the 4 inch light disc from the first concave mirror (M_1) exactly coincides with M_2; if not, adjustment the first concave mirror (M_1) by turning the three adjusting screws at the end of the box.

4) Second Concave Mirror M_2: (Refer to Fig. 4)

The adjustment of the second concave mirror (M_2) can be done in the same way; a small white cardboard is inserted between M_2 and the third diagonal Mirror (D_3) to see if the pencil light from the mirror M_2 impinges at the center of the third diagonal mirror.

5) Focusing the Second Concave Mirror (M_2): (Refer to Fig. 7)

Place a small ground glass at the plane of the knife edge and move the third diagonal mirror by turning the focusing knob K_1 to make a sharp image of the light source slit on the ground glass. The sharpness of the image can be examined by a magnifying glass. If the image is not at the center of the knife edge, horizontal and vertical adjustment is possible by turning the knobs K_2 & K_3.

6) Checking the Parallelism of the Knife-edge and Image: (Refer to Fig. 9)

Put the high power viewing telescope in place, replace the eyepiece with the 5 x 11 calibration telescope to see if the image of the light source is parallel to the straight knife edge; if not, turn the knife edge.

VI. APPENDIX II

EFFECTIVE INSTRUMENT USE

Configuration of Light Source:

For an effectively circular light source, such as an illuminated pinhole, the rays which contribute to the greatest sensitivity of the system pass through the region of the light source image near the knife edge. Thus rays initially passing through this point have to be refracted upward only slightly in order for them to pass over the knife edge and contribute to the illumination on the viewing screen. On the other hand, those rays which pass through the lower part of the light source image away from the knife edge must undergo a large refraction in the region T of Fig. 1 before they can contribute to the screen illumination. For the maximum sensitivity, therefore, the maximum number of rays in the light source image must lie close to the knife edge. This requirement is most easily satisfied by the use of a slit source of light. Here, no rays lie at a large distance from the edge itself; consequently, more of the rays can be bent over the knife edge for a given amount of refraction in the striation as shown in Fig. 40-a.

The Image of Light Source:

A requirement for maximum sensitivity is that the light source image adjacent to the knife edge be as straight

and as sharply defined as possible. Then it will conform to the sharp edge of the knife edge so that accurate positioning of the knife edge can be made with respect to the image. Of the sharpness of the image of the light source there are two factors:

a) the quality of the optical parts; and

b) the types of optical set-up. (Refer to (1) in Bibliography)

The Orientation of Knife-edge:

If the index of refraction gradient lies only in a horizontal plane, thereby producing a corresponding refraction in that plane, the effect is to produce a lateral shift of an affected ray parallel to the knife edge. Such a displacement, if strictly parallel to the edge, cannot affect the viewing screen illumination. (See Fig.40-b) It can be seen, therefore, that a further requirement for maximum sensitivity of the system is that the effective light source, its image, and the knife edge must be perpendicular to the index of refraction gradient being considered.(See Fig.40-c)

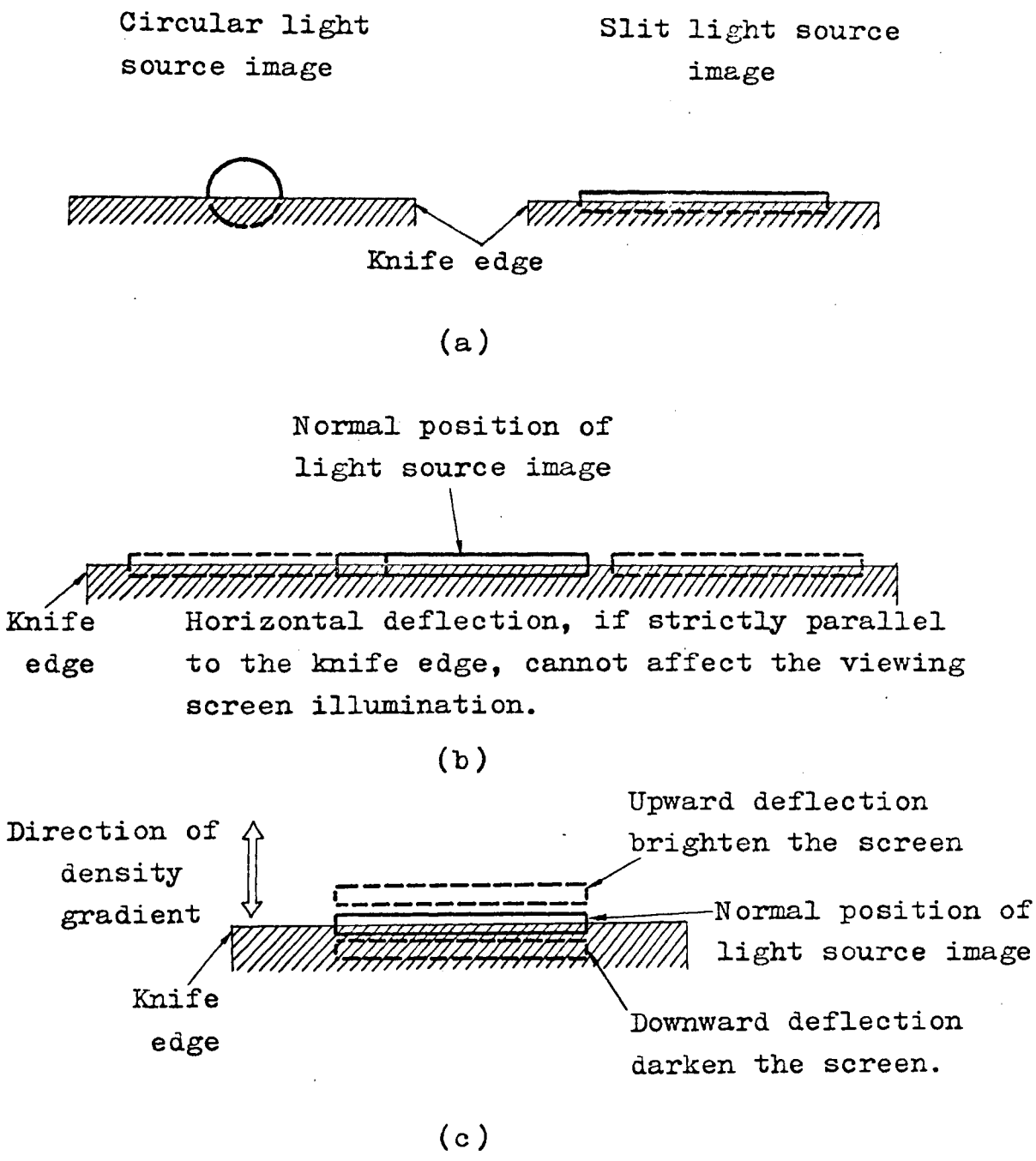

Fig. 40. (a) Configuration of light source and light source image. (b),(c) Orientation of knife edge.

Critical deflection angle:

The deflection angle of light source image is very critical when the schlieren system is working at high sensitivity, because if the deflection angle is larger than the critical angle the illumination of the test section would be constant. This can be best shown in the following diagram.

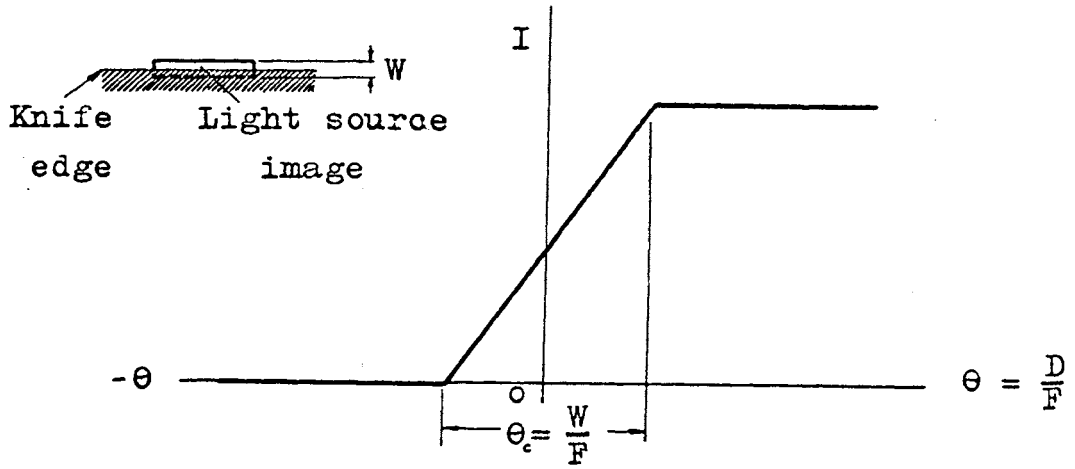

Fig. 41. Critical deflection angle.

Where I = Test section illumination.

W = Width of light source image.

D = Deflection.

F = Focal length of concave mirror M_2.

θ = Deflection angle.

θ_c = Critical deflection angle.

If high sensitivity is desired, the critical deflection angle should be made as small as possible.

VII. VITA

The author, Philip Ling Chen, was born on January 23, 1936 in Nanking, China. He received both his high school and college education in Taipei, Taiwan, China. A Bachelor of Science Degree in Mechanical Engineering was received from National Taiwan University in June 1959. Following graduation he was called to the services of the Chinese Navy. After a year and half of duty with the Navy, he taught in his Alma Mater as a teaching assistant. In September of 1963, he left his work and came to this country to pursue his studies toward a Master of Science degree in Mechanical Engineering at the University of Missouri at Rolla.